



**Michigan
Technological
University**

Michigan Technological University
Digital Commons @ Michigan Tech

Michigan Tech Publications

4-13-2022

Sources of Hydrothermal Fluids Inferred from Oxygen and Carbon Isotope Composition of Calcite, Keweenaw Peninsula Native Copper District, Michigan, USA

Thomas Bodden
Michigan Technological University, tjbodden@mtu.edu

Theodore J. Bornhorst
Michigan Technological University, tjb@mtu.edu

Florence Bégué
Université de Genève

Chad Deering
Michigan Technological University, cddeering@mtu.edu

Follow this and additional works at: <https://digitalcommons.mtu.edu/michigantech-p>



Part of the [Geological Engineering Commons](#), and the [Mining Engineering Commons](#)

Recommended Citation

Bodden, T., Bornhorst, T. J., Bégué, F., & Deering, C. (2022). Sources of Hydrothermal Fluids Inferred from Oxygen and Carbon Isotope Composition of Calcite, Keweenaw Peninsula Native Copper District, Michigan, USA. *Minerals*, 12(4). <http://doi.org/10.3390/min12040474>
Retrieved from: <https://digitalcommons.mtu.edu/michigantech-p/15932>


Follow this and additional works at: <https://digitalcommons.mtu.edu/michigantech-p>



Part of the [Geological Engineering Commons](#), and the [Mining Engineering Commons](#)

Review

Sources of Hydrothermal Fluids Inferred from Oxygen and Carbon Isotope Composition of Calcite, Keweenaw Peninsula Native Copper District, Michigan, USA

Thomas J. Bodden¹, Theodore J. Bornhorst^{1,2,*} , Florence Bégué³ and Chad Deering¹

¹ Department of Geological and Mining Engineering and Sciences, Michigan Technological University, Houghton, MI 49931, USA; tjbodden@mtu.edu (T.J.B.); cddeerin@mtu.edu (C.D.)

² A. E. Seaman Mineral Museum, Michigan Technological University, Houghton, MI 49931, USA

³ Department of Earth Sciences, University of Geneva, 1205 Geneva, Switzerland; florence.begue@unige.ch

* Correspondence: tjb@mtu.edu

Abstract: The Mesoproterozoic North American Midcontinent Rift hosts the world's largest accumulation of native copper in Michigan's Keweenaw Peninsula. During a regional metamorphogenic-hydrothermal event, native copper was deposited along with spatially zoned main-stage minerals in a thermal high. This was followed by deposition of late-stage minerals including minor copper sulfide. Inferences from the oxygen and carbon isotopic composition of main-stage hydrothermal fluids, as calculated from 296 new and compiled isotopic measurements on calcite, are consistent with existing models that low-sulfur saline native copper ore-forming fluids were dominantly derived by burial metamorphic processes from the very low sulfur basalt-dominated rift fill at depth below the native copper deposits. Co-variation of oxygen and carbon isotopic compositions are consistent with mixing of metamorphic-derived fluids with two additional isotopically different fluids. One of these is proposed to be evolved seawater that provided an outside source of salinity. This fluid mixed at depth and participated in the formation of a well-mixed hybrid metamorphic-dominated ore-forming fluid. Secondary Ion Mass Spectrometry in-situ isotopic analyses of calcite demonstrate a high degree of variability within samples that is attributed to variable degrees of shallow mixing of the hybrid ore-forming fluid with sulfur-poor, reduced evolved meteoric water in the zone of precipitation. The oxygen and carbon isotopic compositions of 100 new and compiled measurements on late-stage calcite are mostly isotopically different than the main-stage hydrothermal fluids. The late-stage hydrothermal fluids are interpreted as various proportions of mixing of evolved meteoric water, main-stage hybrid ore-forming fluid, and shallow, evolved seawater in the relatively shallow zone of precipitation.

Keywords: native copper; oxygen and carbon isotopes; Keweenaw Peninsula; Michigan; burial metamorphism; fluid mixing; ore genesis



Citation: Bodden, T.J.; Bornhorst, T.J.; Bégué, F.; Deering, C. Sources of Hydrothermal Fluids Inferred from Oxygen and Carbon Isotope Composition of Calcite, Keweenaw Peninsula Native Copper District, Michigan, USA. *Minerals* **2022**, *12*, 474. <https://doi.org/10.3390/min12040474>

Academic Editors: Vasiliios Melfos, Panagiotis Voudouris and Grigorios Aarne Sakellaris

Received: 11 March 2022

Accepted: 10 April 2022

Published: 13 April 2022

Publisher's Note: MDPI stays neutral with regard to jurisdictional claims in published maps and institutional affiliations.



Copyright: © 2022 by the authors. Licensee MDPI, Basel, Switzerland. This article is an open access article distributed under the terms and conditions of the Creative Commons Attribution (CC BY) license (<https://creativecommons.org/licenses/by/4.0/>).

1. Introduction

The copper deposits of the Keweenaw Peninsula native copper district contain the world's largest accumulation of native copper. They are notable for consisting of almost entirely native copper; the deposits produced 5 billion kg of refined copper from 1845 to 1968 [1,2]. The first major mining rush in North America in the early to mid-1840s to the Keweenaw Peninsula was sparked by an 1841 geologic report written by Douglass Houghton, Michigan's first state geologist [3]. A major geologic study in the 1920s culminated with publication of U.S. Geological Survey Professional Paper 144 [4]. Just before commercial mining ended and the underground mines left to flood, U.S. Geological Survey geologist, White, published a district-wide review including a detailed analysis of current thinking on genetic models [5]. The district has not benefited as much as elsewhere from the explosion in modern analytical methods in the last 50 years.

There is a long history elsewhere of using light stable isotopes to determine hydrothermal fluid sources. Only two previous light stable isotope studies have been published on the Keweenaw Peninsula native copper district [6,7]. These studies supported the long-standing hypothesis that the native copper ore-forming hydrothermal fluids were dominantly generated by burial metamorphic processes [5–9]. However, these two studies also differed in the possible involvement of seawater and magmatic waters in the ore-forming hydrothermal fluids. Bornhorst and Woodruff [10] used light stable isotopes to propose fluid mixing as an important process to help explain isotopic variability. We initiated this light stable isotope study to evaluate fluid mixing, but subsequently expanded the scope to the sources of hydrothermal fluids. We have compiled 157 district-wide bulk oxygen and carbon stable isotope data on calcite from published studies and added 239 new oxygen and carbon spot analyses by Secondary Ion Mass Spectrometry (SIMS) from a select number of samples. The new data are provided in the Supplementary Materials to this publication. District-scale inferences of the nature of the hydrothermal fluids of the Keweenaw Peninsula native copper district are the focus of this publication.

2. Geologic Setting

The Midcontinent Rift system extends over 2000 km from Kansas to Lake Superior (Figure 1). The rift-related rocks were deposited between 1.15 to 0.95 Ga [11–13]. About 25 km of the Mesoproterozoic basalt-dominated rift-filling section is overlain by about 8 km of clastic sedimentary rocks and are largely hidden beneath the center of Lake Superior northwest of the Keweenaw Peninsula. Rift-related rocks are exposed around the Lake Superior region (Figure 1). On the Keweenaw Peninsula, the exposed rift-filling basalt-dominated Portage Lake Volcanics (PLV) section is about 5 km thick with the base of the section truncated by the reverse Keweenaw Fault (Figure 2). The PLV was deposited between about 1098 to 1092 Ma [14]. Exposed on the eastern and southern edge of the Jacobsville Sandstone basin, the stratigraphically older volcanics of the Powder Mill Group were deposited from about 1098 to 1100 Ma [15]. The PLV is composed of about 200 subaerial basalt flows, a few rhyolite flow-dome-horizons and intrusives near the base of the exposed section, and scattered interflow clastic sedimentary rock layers [4,5,16,17]. The subaerial basalt lava flows consist of a massive interior capped by an amygdaloidal and/or brecciated flow top; typically flows are around 10 to 20 m thick. Brecciated flow tops generally have higher porosity than amygdaloidal flow tops and are better ore host rocks. The interflow clastic sedimentary rocks within the PLV range from a few cm up to 40 m thick and consist of red-colored conglomerate with lesser amounts of interbedded, red-colored sandstone and sometimes red-colored siltstone and shale [5]. The conglomerate consists of pebble-sized to boulder-sized clasts of rift-related volcanic rocks that are sub-rounded to angular in texture. The clasts are dominantly felsic, though they range from mafic to felsic compositions.

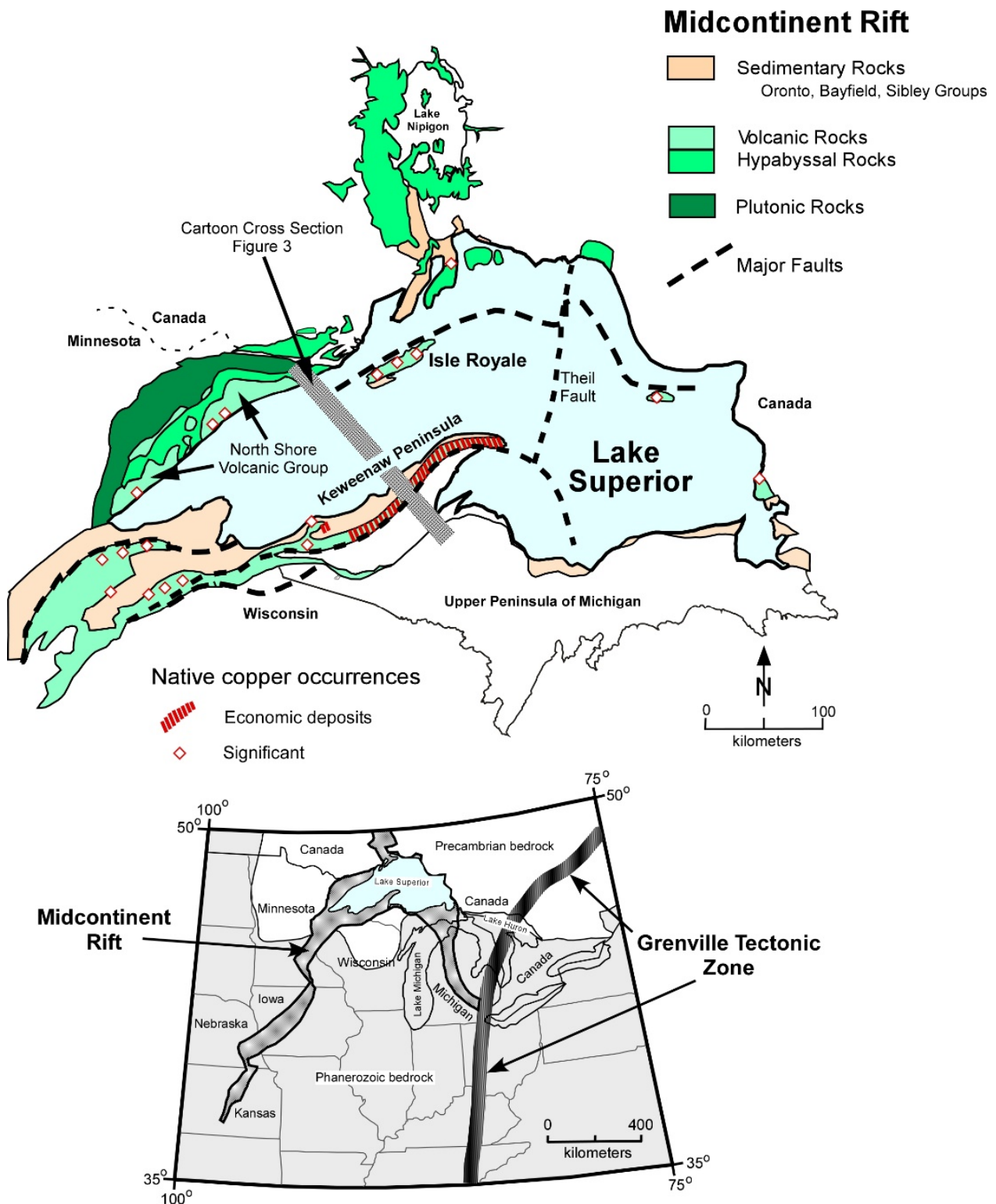
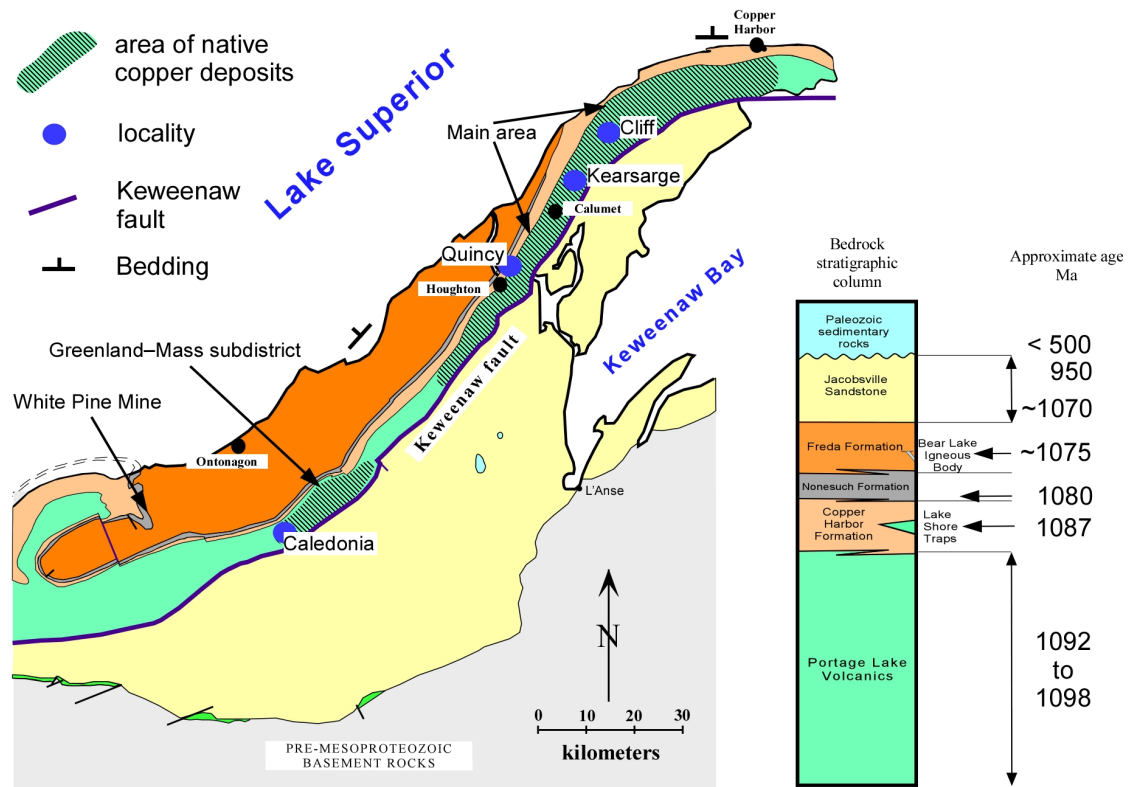


Figure 1. Geologic setting of the Mesoproterozoic Midcontinent Rift showing area of economic native copper deposits in the Keweenaw Peninsula and occurrences of native copper in exposed rocks of the Midcontinent Rift. The insert shows the front of the Grenville tectonic zone, a continent-continent suture that resulted in compression late in the history of the rift. Modified from Bornhorst and Lankton [2].

A. Geologic Map Keweenaw Peninsula Native Copper District



B. Main-Stage Hydrothermal Mineral Zones

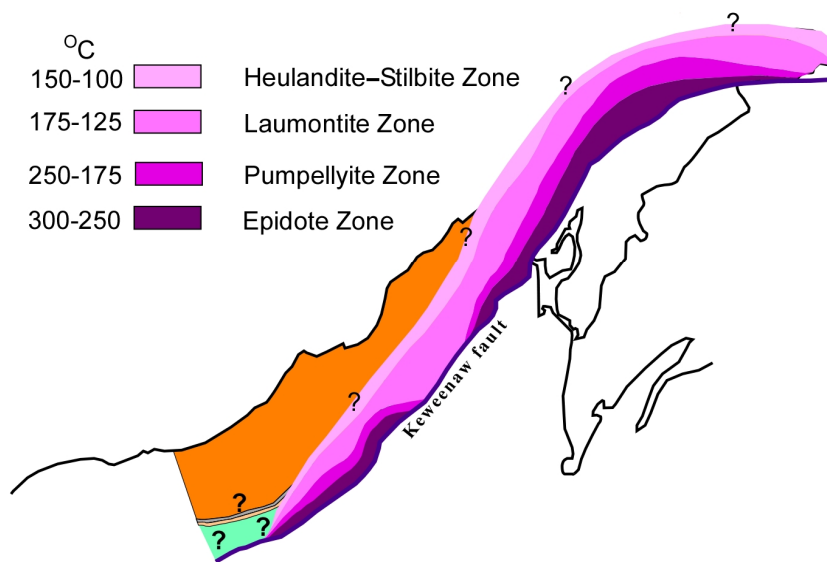


Figure 2. (A) Bedrock geologic map of the Keweenaw Peninsula native copper district showing the main-area of native copper deposits and the Greenland-Mass subdistrict, which is a smaller area hosting native copper deposits. The district extends to the White Pine Mine where late-stage native copper cross cuts the shale-hosted diagenetic chalcocite deposit. Sampling localities shown with blue dot, towns with black dot. (B) Map showing main-stage hydrothermal mineral zones and temperatures discussed in the text. The Jacobsville Sandstone is not shown since the main-stage hydrothermal/metamorphic event pre-dated deposition of surface exposures. Modified from Bodden [18].

The clastic sedimentary rocks directly overlying the PLV are red-colored conglomerate and sandstone of the Copper Harbor Formation with abundant calcite cement and exposed thicknesses of up to 2000 m (Figure 2). They were deposited in a semi-arid to arid climate [19] in alluvial fans extending into the rift [20]. There is an interval of basaltic subaerial lava flows (Lake Shore Traps) within the Copper Harbor Formation deposited about 1087 Ma [14]. The Copper Harbor Formation is conformably overlain by gray to black siltstone and shale of the Nonesuch Formation with exposed thickness of up to 215 m where it is overlain by the Freda Formation [21]. The Nonesuch Formation was deposited about 1080 Ma [22]. The depositional setting of the Nonesuch Formation has been proposed as either lacustrine or marine [21]. However, recent studies support the interpretation that the Nonesuch was deposited in a shallow marine embayment or marine-influenced estuarine system [23,24]. In addition, Jones et al. [22] have suggested that all of the Copper Harbor Formation is part of a “braided fluvial-evaporitic shoreline-marine embayment triplet” and not non-marine as previously interpreted. This marine related interpretation is consistent with long-lasting and extensive incursions of seawater into the rift during the extended period of clastic sedimentation following the waning and ending of rift volcanism. The Nonesuch Formation is gradational into overlying fluvial red-colored very fine sandstone, siltstone, and shale of the Freda Formation with exposed thicknesses of up to 4000 m (Figure 2) and indicates the transition to the end of marine incursions into the rift. The youngest known magmatism in the Midcontinent Rift is a single flow-dome-intrusive body (Bear Lake igneous body) emplaced in the Freda Formation at about 1075 Ma [25].

These rift-filling rocks dip towards the center of the rift as a result of syn-depositional sagging and compression late in the history of the rift (Figures 2 and 3) [2]. A late regional compressional event connected with continental collision along the Grenville tectonic zone beginning at about 1070 to 1040 Ma [26,27] produced many lesser faults and fractures (Figure 1). The reverse Keweenaw fault (Figure 2) was formed by Grenville tectonism with a protracted history from 1070 to 950 Ma [13,28]. The rift-flanking Jacobsville Sandstone consists of fluvial red-to-white-colored sandstone and was likely deposited during the compressional event in association with the protracted development of the Keweenaw fault.

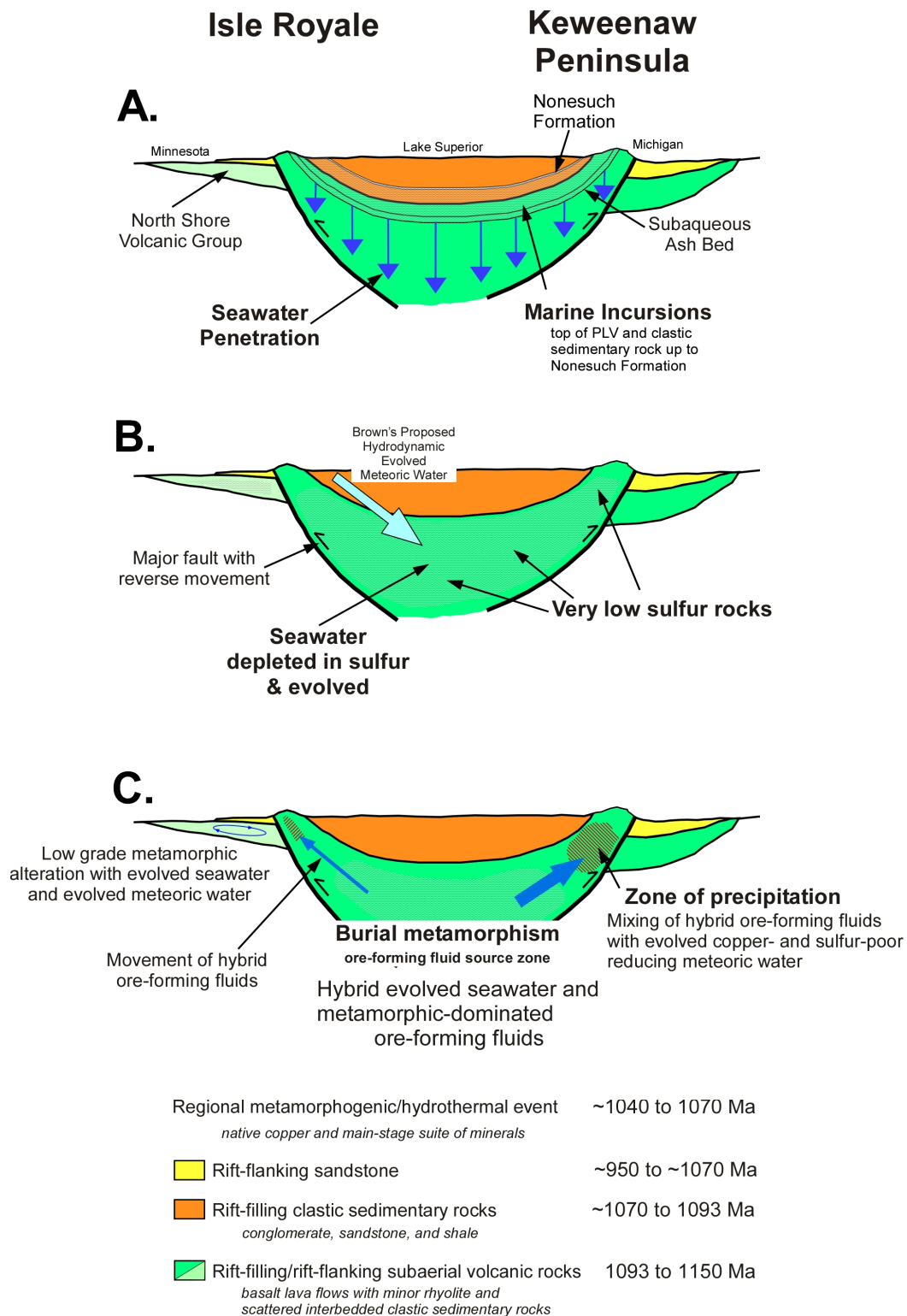


Figure 3. Cartoon geologic cross section illustrating the conceptual genetic model for the native copper deposits of the Keweenaw Peninsula. (A) Depositional infilling of the rift. (B) Initial burial prior to burial metamorphism. (C) Regional hydrothermal event synchronous with regional compression. Cartoon cross section faces north from Isle Royale to the Keweenaw Peninsula. Location shown in Figure 1. Modified from Bornhorst and Mathur [29].

The native copper deposits of the Keweenaw Peninsula were formed during a regional hydrothermal event between about 1070 to 1040 Ma (Figure 3) [30–32]. The age of the regional hydrothermal event is corroborated by radiometric dating from the native copper associated main-stage minerals in the main area of the Keweenaw Peninsula native copper district, native copper and associated minerals that cross cut the sedimentary rock hosted chalcocite deposit at the White Pine Mine, and the main metamorphogenic-hydrothermal event in the North Shore Volcanic Group. Bornhorst [33] proposed that faults and fractures formed during late rift Grenville compression integrated the pathways for movement of ore-forming fluids leading to the formation of the native copper deposits and main-stage minerals. This is consistent with the age of the Keweenaw fault and the regional metamorphic/hydrothermal event from about 1070 to 1040 Ma.

The PLV hosts the most significant deposits of native copper within the tops of sub-aerial lava flows and interflow conglomerates [4,5]. Those occurrences of native copper deposits, from which there has been a production of ~0.5 million kg of copper or more, are concentrated in two separate areas: (1) the main native copper district from South Range to Copper Harbor, and (2) the Greenland-Mass sub-district (Figure 2). About 58.5% of the produced copper is hosted by brecciated and amygdaloidal flow tops, 39.5% by interflow conglomerate and sandstone layers, and 2% by cross-cutting veins [1]. In addition to compression-related faults and fractures, the porosity and permeability of the flow tops and interflow conglomerates facilitate the movement of ore-forming fluids and provide open spaces to be filled with precipitated minerals [4–7,9,34].

Butler and Burbank [4] were the first to provide a comprehensive summary of the hydrothermal minerals within the Keweenaw Peninsula native copper district and their temporal relationship (paragenesis) with each other. Their “ore period” has been subdivided here into two stages of hydrothermal mineral formation: main-stage and late-stage (Figure 4). The precipitation of native copper generally overlaps with all the minerals assigned here to the main-stage, which are interpreted to have formed during the same continuous hydrothermal event.

While widespread, the volumetrically minor late-stage hydrothermal minerals tend to be localized; late-stage minerals are more frequent along thin fractures and faults that cut across native copper mineralization. The late-stage minerals are notably more abundant near the Keweenaw fault in structurally disturbed PLV. Main-stage alteration minerals are notably less abundant adjacent to the Keweenaw fault. This indicates that the Keweenaw fault was not a principal pathway for localizing the main-stage native copper deposits. The late-stage assemblage includes very minor copper sulfide minerals (Figure 4). Bornhorst and Suchoski [35] have shown that even a very small amount of sulfur in the hydrothermal fluids would likely lead to precipitation of copper sulfide minerals rather than native copper, suggesting that the late-stage minerals are precipitated from fluids of a different source. The suite of late-stage minerals is indicative of temperatures of formation less than the main-stage minerals within the native copper district [7]. While late-stage mineralization occurs temporally after the main-stage it is generally assumed to be part of a single continuous hydrothermal event, although the absolute age range of the late-stage event in the Keweenaw Peninsula is unknown. A late calcite vein at the White Pine mine was dated at about 1000 to 1040 Ma [32] on the low end of the likely age of main-stage hydrothermal activity in the Keweenaw Peninsula but compatible with a continuous late-stage hydrothermal activity. Schmidt [31] dated a paragenetic late mineral assemblage in the North Shore Volcanic Group to be about 945 to 965 Ma; this event occurred well after the main-stage native copper forming event, and if the late-stage of the Keweenaw Peninsula is continuous with the main-stage, then the 945 to 965 Ma event may represent a pulse of hydrothermal activity after the late-stage of the Keweenaw Peninsula and perhaps not yet recognized as being present in the Keweenaw Peninsula.

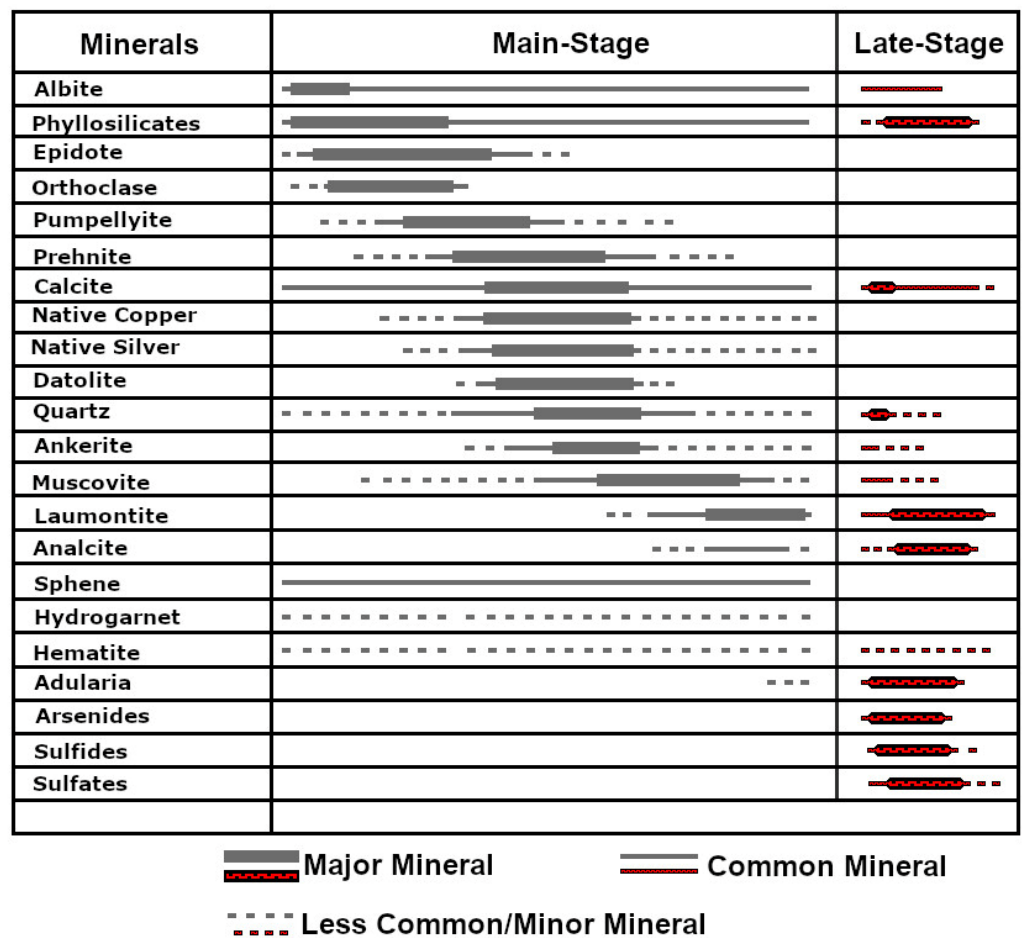


Figure 4. Paragenesis of mineral formation within the Keweenaw Peninsula native copper district. Modified from [4,18].

3. Mineral Zones and Temperature of Precipitation

The main-stage minerals occur as spatially separable mineral zones that reflect district wide and regional variations in the fluid composition and/or conditions of mineralization (Figure 2). In contrast, the late-stage minerals are not zoned but are similar throughout the native copper district. Stoiber and Davidson [34] were the first to describe the regional pattern of main-stage hydrothermal mineral zoning within the PLV based on the mineral distribution in stratigraphic sections of drill cores and within mines. They used the presence or absence of prehnite, epidote and quartz to mark a line of occurrence, and showed that mineral zones of the native copper district cross cut the strike of the PLV. Later, Jolly and Smith [9] subdivided the main-stage hydrothermal mineral assemblages within the PLV in a single cross-section of stepped drill cores into three low-grade “burial metamorphic” zones of decreasing grade: epidote zone, pumpellyite zone, and laumontite zone. Subsequently, Livnat [6] provided additional information on spatial zonation of the minerals and showed that mineral zones dip more shallowly than the strata of the PLV.

The metamorphogenic-hydrothermal mineral assemblages for the North Shore Volcanic Group of Minnesota (Figure 1) [36] are mineralogically similar to those of the PLV [6,9] and of similar age [31]. The North Shore Volcanic Group is a rift-related Mesoproterozoic basalt-dominated formation that is stratigraphically beneath the PLV. The main-stage hydrothermal mineral assemblages of the Keweenaw Peninsula can be readily subdivided into the mineral zones used by Schmidt [36] from highest to lowest grade: (1) the epidote zone characterized by actinolite (not found in the Keweenaw Peninsula), epidote, pumpellyite, prehnite, chlorite, and garnet; (2) the pumpellyite zone characterized by epidote, pumpellyite, prehnite, traces of laumontite, chlorite, potential garnet and corrensite,

and (3) the laumontite zone characterized by laumontite, chlorite, calcite, phyllosilicates (corrensite), epistilbite, and quartz. Two of Schmidt's [36] zones occur on the Keweenaw Peninsula but are located outside of the native copper district: the heulandite-stilbite zone characterized by laumontite, calcite, phyllosilicates (smectite), heulandite, stilbite, scolecite, mordenite, and epistilbite, and a lower grade thomsonite-scolecite-smectite zone characterized by smectite, thomsonite, calcite, heulandite, scolecite and quartz. Only minerals temporally/genetically related to each other, e.g., main-stage minerals (Figure 4), can be mapped together. We have created a mineral zonation map based on our analysis of the spatial distribution of the main-stage hydrothermal mineral assemblages within the native copper district (Figure 2).

Livnat [6] proposed formation temperatures for the mineral zones mostly based on temperatures of formation of metamorphic mineral assemblages supplemented with stable isotope geothermometry. Püschner [7] applied a chlorite geothermometer to help estimate the formation temperatures. Their main-stage mineral temperatures of formation are consistent with Schmidt's [36] inferred temperatures. Based on these data, we estimate the main-stage formation temperatures for the epidote zone to be 275 ± 25 °C, the pumpellyite zone to be $200\text{--}225 \pm 25$ °C, and the laumontite zone to be 150 ± 25 °C. The mapped mineral zones cross cut the strike of the PLV near the tip of the Keweenaw Peninsula and southwest of the main area of native copper deposits, and on either side of the Greenland-Mass subdistrict (Figure 2). Since the mineral zones can be equated with temperature, the spatial distribution fits with a district-wide hydrothermal thermal high coincident with the more significant native copper deposits.

The Keweenaw Peninsula late-stage mineral assemblage (Figure 3) is similar to the laumontite and heulandite-stilbite zones of Schmidt [36]. The heulandite-stilbite zone is interpreted to have formed at temperatures of <150 °C, whereas the laumontite zone formation temperature is slightly higher. The estimated late-stage mineral formation temperature is 125 ± 25 °C. Within the main area of the native copper district and the Greenland-Mass subdistrict (Figure 2), the main-stage minerals are readily distinguished from the late-stage minerals. Outside these areas, identifying the late-stage mineral assemblage is difficult because the predicted main-stage mineral assemblage would be more or less the same as the late-stage. Thus, the light stable isotope data in this publication are restricted to the main area of the district and the subdistrict.

4. Methods

4.1. Compilation

This study focuses on the oxygen and carbon isotopic composition of calcite. We compiled 84 bulk analyses collected by Livnat [6], 41 bulk analyses collected by Bornhorst and Woodruff [10], and 32 bulk analyses collected by Püschner [7] for a total of 157 sets of oxygen and carbon stable isotope analyses on calcite from the native copper district. Each analysis was assigned to either main-stage or late-stage hydrothermal evolution; those samples of uncertain stage are excluded from the compilation. Additional oxygen stable isotope analyses of chlorite/clinocllore and quartz were compiled by Bodden [18] from Livnat [6] and Püschner [7] for comparison with the calcite data.

All previously published stable isotope data were collected via a bulk analysis method. For calcite, typically a small amount of powder is dissolved in acid (likely anhydrous phosphoric acid) and the resulting CO₂ gas is analyzed for oxygen and carbon isotopes by a mass spectrometer. Analytical error for these bulk calcite analyses is assumed to be about $\pm 0.2\%$. Livnat [6] analyzed his samples at the U.S. Geological Survey Isotope Geology Laboratory in Denver, Colorado. Livnat's [6] oxygen isotopes were analyzed using extraction methods after McCrea [37]. Püschner's [7] stable isotope analyses were done at the stable isotope lab of the Geological Department of Earth and Atmospheric Sciences at the Indiana University at Bloomington.

4.2. New Data by Secondary Ion Mass Spectrometry

Eight calcite samples from the native copper district, six main-stage and two late-stage, were analyzed for this study with Secondary Ion Mass Spectrometry (SIMS) at the Swiss SIMS national facility (University of Lausanne, Switzerland) for oxygen and carbon isotope compositions. The samples were selected from the Keweenaw Research Collection of the A. E. Seaman Mineral Museum to be representative of the deposits of the native copper district. Two deposits, the Quincy mine (Pewabic flow tops) and Kearsarge flow-top deposits (with multiple mine names), are large deposits in the main part of the native copper district. One deposit, the Caledonia mine, is in the Greenland-Mass subdistrict (Figure 2). From the Pewabic deposit, the fourth largest deposit in the district, three samples were analyzed; these were collected underground. Two of the samples were vug-filling calcite crystals with inclusions of native copper and the other consisted of open-space filling main-stage minerals. The calcite crystals were sectioned perpendicular to the C-axis to provide coverage of growth zones during the history of crystal formation. From the Kearsarge deposit, the second largest deposit in the district, two samples were analyzed; both were collected underground when the mines were still operating. One of these consisted of main-stage minerals including calcite, whereas the other is a late-stage cross-cutting calcite, laumontite, and natrolite vein. From the Caledonia mine, two samples were analyzed; these samples were collected underground as shallow levels of this mine are above the water table and are accessible. One of these consists of open-space filling main-stage minerals and the other is a late-stage calcite and laumontite vein which cross cuts native copper mineralization.

SIMS is an in-situ analytical technique used to analyze the mass ratios of secondary ions with the process of hitting the surface of the calcite with a focused ion beam. The same analytical settings for in-situ analyses by SIMS of carbonate material were used as described in more detail by Bégué et al. [38]. Polished thin sections of the selected samples for SIMS analysis were imaged by optical cathodoluminescence (CL) using a cold cathode ERI-MRTEch mounted on a petrological microscope with a voltage of about 8 kV and a current of 0.4 mA (available at the UNIL). Differences in the CL signal of calcite are related to small concentrations of Mn in calcite, which ranges from 0–5000 ppm (Supplementary Materials). These images were used to select areas with multiple calcite generations for SIMS analysis. Thick sections were then cut using a diamond wire saw and pressed into indium mounts, along with a calcite (ZI01; $\delta^{18}\text{O} = 18.29\text{‰} \pm 0.07 \text{ 1SD}$; $\delta^{13}\text{C} = 0.64\text{‰} \pm 0.04 \text{ 1SD}$) and a rhodochrosite standard ($\delta^{18}\text{O} = 18.64\text{‰} \pm 0.04 \text{ 1SD}$; $\delta^{13}\text{C} = 2.83\text{‰} \pm 0.08 \text{ 1SD}$). Both standards were used to correct for the matrix effect associated with Mn content in calcite. We used a Bruker Contour GTK white light interferometric microscope to check that the sample topography was less than 5 μm and, before analysis, the sample surface was made conductive with a 30–35 nm gold coating.

Oxygen and carbon isotopes were measured on a CAMECA IMS 1280HR large radius multi-collector SIMS using a 10 kV and about 1.5 nA primary beam of Cs^+ ions in a Gaussian mode. An electron flood gun compensated the charge build-up at the sample surface. Oxygen isotopes were measured during three analytical sessions. ^{16}O and ^{18}O secondary ions were analyzed at 2460 mass resolving power and collected on two Faraday cups in multi-collection mode, which were calibrated at the beginning of each session (typically 8–12 h). Each analysis took less than 4 min, including 30 s of pre-sputtering to remove the coating and automated centering of secondary ions. Carbon isotopes were also analyzed during three analytical sessions, where ^{12}C and ^{13}C were collected simultaneously on a Faraday cup and an electron multiplier, respectively, with a mass resolving power of ~ 4400 . The pre-sputtering time was 45 s. The spot size for oxygen isotope measurements was between 12 and 15 μm and for carbon isotope measurements about 18–20 μm with a 10 μm raster.

Calcite and rhodochrosite standards were used to correct for instrumental bias due to matrix effect and for machine drift during the analytical session. Each session was started and ended by multiple standard analyses. The calcite standard was also analyzed following every three unknowns, and the rhodochrosite following every six analyses of the

unknowns. A polynomial fit on the calcite standard measurements over the entire session was applied to correct for machine drift over time. Calcite analyses were corrected for their mole fraction of Mn (XMn) where $XMn = Mn / (Ca + Mn)$, using a linear regression between the calcite and the rhodochrosite instrumental mass fractionation. Due to low XMn, matrix effects were small.

The standard reproducibility for oxygen isotopes at the beginning of each session on six analyses was $<0.44\text{‰}$ and $<1.2\text{‰}$ (2SD) for carbon isotopes. Over the whole session standard reproducibility was between 0.21‰ and 0.45‰ (2SD) for oxygen, and between 1.16‰ and 1.29‰ (2SD) for carbon isotopes. The location of the spots was determined based on textural information from the CL images of the calcites and were overlain on the images following the georeferencing method of Linzmeier et al. [39] in QGIS. All data and additional details about the samples are provided in the Supplement for this publication. We report isotope ratios in delta notation (in ‰), relative to Vienna Standard Mean Ocean Water (VSMOW) for oxygen and Vienna Pee Dee Belemnite (VPDB) for carbon isotopes.

The XMn of calcite was determined by electron microprobe analysis (EPMA) with a JEOL JXA-8530F Hyperprobe available at UNIL. An analysis was acquired next to every SIMS spot (20–30 μm offset) using an acceleration voltage of 15 kV, a beam current of 10 nA and a defocused beam of 5 μm . Counting times were 30/15 s (peak/background) for Ca and Mg and 60/30 s for Fe and Mn, using natural carbonates and silicates as standard materials.

The SIMS data are provided in the Supplement for this publication. The 2SD analytical uncertainty for these new data has a median of about $\pm 0.35\text{‰}$ for measured $\delta^{18}\text{O}$ and $\pm 0.65\text{‰}$ for measured $\delta^{13}\text{C}$.

4.3. Mineral-Fluid Fractionation

The stable isotopic composition of a hydrothermal mineral depends on the stable isotopic composition of the fluid from which it precipitated, the temperature of precipitation, and the fractionation factor, i.e., a temperature dependent isotopic fractionation between the fluid and the mineral. Calcite is present in every hydrothermal zone, the main-stage (Figures 2 and 4) and the late-stage. For relevant comparison of the data and discussion on spatial and temporal variation of fluid source, and assuming that calcite precipitated in equilibrium with the fluid, we calculated the isotopic values of the fluid using the independently estimated temperatures [18] of the hydrothermal/metamorphic zone (Figure 2) in which the calcite precipitated. The fractionation equation for different minerals has been determined by laboratory experiments. (T is temperature in Kelvin for all equations).

The $\delta^{18}\text{O}_{\text{H}_2\text{O}}$ fractionation equation for calcite as discussed by O'Neil et al. [40] and later corrected in Friedman and O'Neil [41] is:

$$(\delta^{18}\text{O}_{\text{H}_2\text{O}} \text{‰}) = (\delta^{18}\text{O} \text{‰ of calcite}) - ((2.78 \times 10^6)/T^2) + 2.89 \quad (1)$$

The $\delta^{13}\text{C}_{\text{CO}_2}$ fractionation equation for calcite as discussed by Sheele and Hoefs [42] is

$$(\delta^{13}\text{C}_{\text{CO}_2} \text{‰}) = (\delta^{13}\text{C} \text{‰ of calcite}) - ((3.46 \times 10^6)/T^2) + ((9.58 \times 10^3)/T) - 2.72 \quad (2)$$

The isotopic composition of the hydrothermal fluids as calculated using measured isotopic values in calcite is represented as $\delta^{18}\text{O}_{\text{H}_2\text{O}}$ and $\delta^{13}\text{C}_{\text{CO}_2}$ throughout this paper. The analytical error for the bulk analyses is about $\pm 0.2\text{‰}$ for both $\delta^{18}\text{O}$ and $\delta^{13}\text{C}$. For the SIMS spot analyses 2SE is about $\pm 0.35\text{‰}$ for $\delta^{18}\text{O}$ and $\pm 0.65\text{‰}$ for $\delta^{13}\text{C}$.

The values were calculated using the midpoint of the temperature range for the mineral zone in which a particular sample was located. Thus, there is uncertainty in the temperature of precipitation used to calculate $\delta^{18}\text{O}_{\text{H}_2\text{O}}$ and $\delta^{13}\text{C}_{\text{CO}_2}$ between samples but much less within calcite samples used for SIMS analyses. The temperature uncertainty within mineral zones (Figure 2) is about $\pm 25\text{ °C}$. The high uncertainty in calculated $\delta^{18}\text{O}_{\text{H}_2\text{O}}$ and $\delta^{13}\text{C}_{\text{CO}_2}$ was estimated for our data by calculation at different temperatures. For a main-stage temperature of 212.5 °C (pumpellyite zone) $\pm 25\text{ °C}$, the temperature uncertainty

for $\delta^{18}\text{O}_{\text{H}_2\text{O}}$ is about $\pm 1.2\text{‰}$ and $\delta^{13}\text{C}_{\text{CO}_2}$ is about $\pm 0.6\text{‰}$. For a late-stage temperature of $125 \pm 25\text{ °C}$, the temperature uncertainty for $\delta^{18}\text{O}_{\text{H}_2\text{O}}$ is about $\pm 2.2\text{‰}$ and $\delta^{13}\text{C}_{\text{CO}_2}$ is about $\pm 1.2\text{‰}$. At least some of the heterogeneity of the data is due to the uncertainty in the temperature used to calculate $\delta^{18}\text{O}_{\text{H}_2\text{O}}$ and $\delta^{13}\text{C}_{\text{CO}_2}$. However, it is likely for normally distributed data that most values are nearer the midpoint temperature. We conclude that temperature uncertainty can only explain a limited amount of the isotopic variability and does not change our generalized interpretation of the data.

For oxygen, the isotope composition of the fluid was directly calculated from the raw calcite value using the fractionation equation given above. For carbon, the $\delta^{13}\text{C}_{\text{CO}_2}$ can also be calculated with the fractionation equation given above; however, the carbon isotope composition of the fluid depends not only on the temperature of precipitation but also on the proportion of carbon species in the fluid which depend on, e.g., oxidation state and pH [43]. Livnat [6] concluded that based on the probable conditions, especially his estimate of $\log f_{\text{O}_2}$ of -33 to -26 , during precipitation of native copper in the Keweenaw Peninsula, that $\delta^{13}\text{C}_{\text{CO}_2}$ is approximately equal to $\delta^{13}\text{C}_{\Sigma\text{C}}$ in the fluid.

5. Calcite Oxygen and Carbon Stable Isotope Data

5.1. Bulk Main-Stage

There are 131 bulk oxygen and carbon isotopic analyses of main-stage calcite compiled from the published literature. This large amount of data has a much wider spatial distribution than the new data collected for this study.

For one deposit, the Kearsarge deposit, there are 55 main-stage bulk calcite isotopic analyses, which provide sufficient data to assess the within deposit variability of $\delta^{18}\text{O}_{\text{H}_2\text{O}}$ and $\delta^{13}\text{C}_{\text{CO}_2}$. The Kearsarge deposit is the largest flow-top hosted deposit in the district and the second largest deposit with production of ~ 1 billion kg of refined copper from multiple mines along the productive interval with a strike length of about 13 km, a vertical depth of about 1375 m, and a dip of the deposit between 35° to 40° . Since it is the second largest deposit in the district, it is reasonable to assume that the within-deposit variability is representative, although perhaps greater than others. The large number of samples from the Kearsarge deposit is a result of the focused isotopic study by Bornhorst and Woodruff [10] after their initial evaluation of the degree of isotopic variation represented by 14 analyses published by Livnat [6]. They followed up Livnat's study with 41 additional samples spread out along the strike length of the deposit. They focused on this one deposit to minimize temperature uncertainty. There is considerable within-deposit variation in the main-stage bulk calcite analyses as represented by the Kearsarge deposit, with a range of $\delta^{18}\text{O}_{\text{H}_2\text{O}}$ from $+3.8\text{‰}$ to $+13.4\text{‰}$, and of $\delta^{13}\text{C}_{\text{CO}_2}$ from -2.2‰ to $+1.2\text{‰}$ (Figure 5A).

The other 76 bulk oxygen and carbon isotopic analyses of main-stage calcite are scattered throughout the district; however, there are an insufficient number to assess within, or between, deposit variation. Some are not from the native copper deposits. Important deposits lack any bulk isotopic data. Thus, the current bulk analyses may not capture the entire range of isotopic compositions that would be captured if multiple bulk samples were analyzed from each of the more important deposits. The existing bulk data demonstrate that for the district there is a large degree of main-stage isotopic variation, a range of $\delta^{18}\text{O}_{\text{H}_2\text{O}}$ from $+2.4\text{‰}$ to $+20.4\text{‰}$ and of $\delta^{13}\text{C}_{\text{CO}_2}$ from -4.8‰ to $+3.5\text{‰}$ (Figure 5C). The district-wide variability is larger than observed within the single Kearsarge deposit.

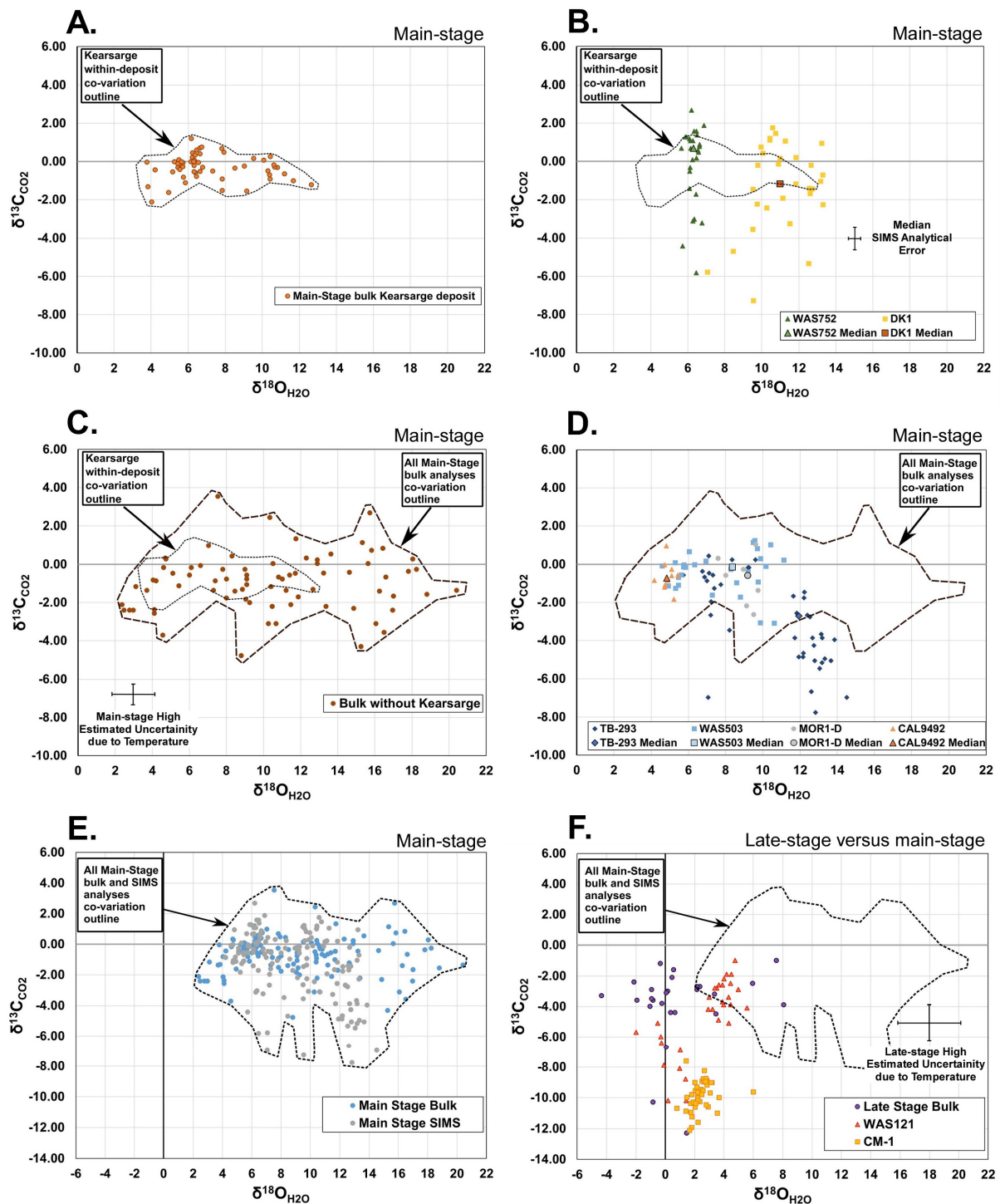


Figure 5. Covariation of carbon and oxygen isotopes in calcite from the Keweenaw Peninsula native copper district. Carbon and oxygen isotopes calculated in terms of CO₂ and H₂O, respectively, as discussed in the text. Analytical and temperature uncertainty shown. (A) Main-stage Kearsarge bulk isotopic composition with field around points. (B) Main-stage Kearsarge bulk isotopic field compared to SIMS data with high within sample variation but median value within the bulk field. (C) Main-stage comparison of Kearsarge bulk isotopic composition and all bulk isotopic data. (D) Main-stage comparison of all bulk isotopic data to SIMS data except Kearsarge. (E) Main-stage all bulk and SIMS isotopic data. (F) Comparison of main-stage to late-stage isotopic composition. Analytical and temperature uncertainty discussed in Section 4.3.

5.2. Main-Stage SIMS Isotopic Compositions

There are 165 spot oxygen and carbon isotopic analyses of main-stage calcite determined for this study from three different deposits. The size of each SIMS spot analysis is between 10 and 30 μm , which is far less than the sample size used for the bulk analysis. For the bulk isotopic analyses, a fraction of the mineral being analyzed was extracted and inspected for purity. After extraction, the samples were hand-crushed and sieved to produce powders of uniform particle size, and were mixed to produce an assumed uniform isotopic composition. Thus, it is expected that the SIMS spot analyses of chips from the same sample would capture some level of within sample variation not captured in the bulk analyses. It is reasonable to expect the within-sample variation of the SIMS spot analyses would be clustered about the bulk value with a regular distribution. For example, the median of the SIMS spot analyses taken from a split of a sample used for bulk analyses should be close to the bulk sample value.

Two samples from the Kearsarge flow were analyzed by SIMS. The median of the two samples analyzed by SIMS fell within the range of the Kearsarge bulk calcite analyses (Figure 5B). The within-sample isotopic variation of both samples exceeded the analytical error. The SIMS data captures variability otherwise not seen due to the averaging effect of the bulk analyses. The SIMS data for DK1 demonstrated a high degree of within sample variation at the sub mm scale. SIMS data are provided in the Supplementary Materials.

The Quincy mine (Pewabic deposit) is the fourth largest deposit in the district. There are no published bulk isotopic analyses from this deposit. Three samples of main-stage calcite samples from the Quincy mine were analyzed by SIMS. Two of these were vug-filling calcite crystals, TB-293 and MOR-1, which were cut perpendicular to the C-axis to be able to analyze successive growth zones during the formation of the crystal. Sample WAS-505 was a massive open-space filling calcite but cathodoluminescence suggested areas of differing calcite growth. The median of the individual spot analyses for each of these three samples fell within the range of the overall main-stage bulk analyses (Figure 5D). TB-293 had a large isotopic variation (Figures 5D and 6), the within sample variation exceeding analytical uncertainty. WAS-505 also had a large isotopic variation. The variation within MOR-1 was modest and less than the other two, although the variation was greater than the analytical uncertainty.

One sample of main-stage calcite from the Caledonia Mine, located in the Greenland-Mass subdistrict was analyzed by SIMS. Its total variation was modest.

The within-sample isotopic variation demonstrated by the SIMS data was within roughly at least plus or minus 1‰ to 3‰ for both $\delta^{13}\text{C}_{\text{CO}_2}$ and $\delta^{18}\text{O}_{\text{H}_2\text{O}}$. This suggests that each bulk data point likely represents a “cloud” of data with this level of within-sample isotopic variation.

There are 296 combined bulk and spot analyses of oxygen and carbon from main-stage calcite. The frequency distribution of the $\delta^{18}\text{O}_{\text{H}_2\text{O}}$ and $\delta^{13}\text{C}_{\text{CO}_2}$ by the two different analytical techniques, bulk and spot by SIMS, were similar to one another. The combined main-stage calcite co-variation had a large range in $\delta^{18}\text{O}_{\text{H}_2\text{O}}$ from +2.36‰ to +20.4‰ and in $\delta^{13}\text{C}_{\text{CO}_2}$ from −7.76‰ to +3.54‰ (Figure 5E). There was a concentration of $\delta^{18}\text{O}_{\text{H}_2\text{O}}$ between about +5‰ to +13‰ and a concentration of $\delta^{13}\text{C}_{\text{CO}_2}$ from about −2‰ to +2‰ (Figure 5E). There was no visual co-variation pattern between $\delta^{18}\text{O}_{\text{H}_2\text{O}}$ and $\delta^{13}\text{C}_{\text{CO}_2}$. Since many deposits have not been isotopically analyzed, it is possible that the combined main-stage calcite data may not adequately distribution of isotopic compositions. The absolute isotopic values of minerals other than calcite from published sources [6,7] are consistent with the calcite analyses [18].

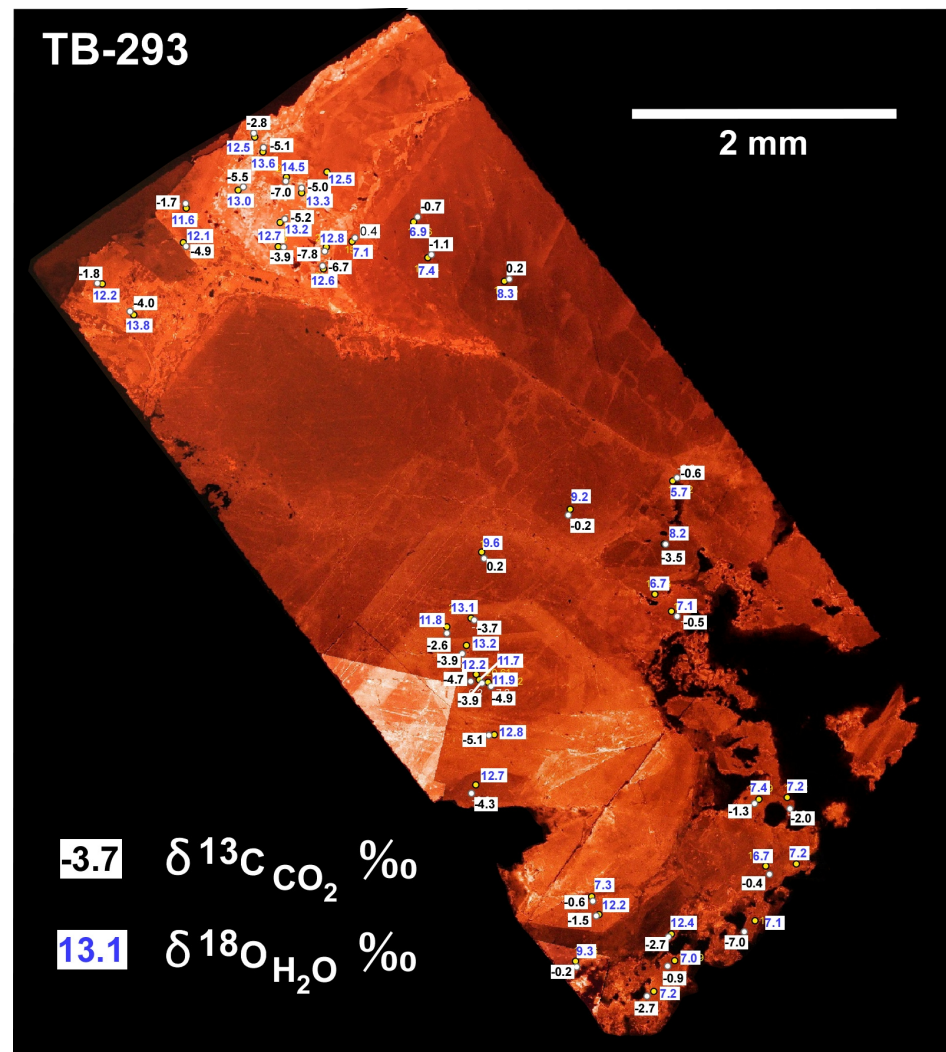


Figure 6. Cathodoluminescence photo of main-stage calcite sample TB-293. TB-293 is a calcite crystal cut perpendicular to the C-axis. Carbon and oxygen isotopic values calculated at constant temperature as $\delta^{18}\text{O}_{\text{H}_2\text{O}}$ and $\delta^{13}\text{C}_{\text{CO}_2}$ are shown for the analytical spot locations. Analytical error discussed in text. Data provided in Supplementary Materials.

5.3. Late-Stage Isotopic Compositions

There are only 26 bulk oxygen and carbon isotopic analyses of late-stage calcite from scattered locations within the native copper district. The 74 spot analyses by SIMS were from two different locations, the Kearsarge deposit and the Caledonia Mine. The frequency distribution for all late-stage $\delta^{18}\text{O}_{\text{H}_2\text{O}}$ is visually approaching a normal distribution. The $\delta^{13}\text{C}_{\text{CO}_2}$ is visually bimodal with two clusters centered about different carbon isotopic values (Figure 5F). Within sample WAS-121, the SIMS data is also distributed in two groups of $\delta^{13}\text{C}_{\text{CO}_2}$. These two groups are also shown by the raw SIMS data (Supplementary Materials) since a constant temperature was used for calculation. The cathodoluminescence response suggests that the two isotopic groups correlate with texturally different calcite with the lower oxygen end-member precipitating later. The co-variation pattern of late-stage $\delta^{18}\text{O}_{\text{H}_2\text{O}}$ and $\delta^{13}\text{C}_{\text{CO}_2}$ is poorly defined (Figure 5F). There was a cluster of data centered about $\delta^{18}\text{O}_{\text{H}_2\text{O}} +4\text{‰}$ and $\delta^{13}\text{C}_{\text{CO}_2} -3\text{‰}$ and a weak visually negative correlation trend from $\delta^{18}\text{O}_{\text{H}_2\text{O}} +3\text{‰}$ and $\delta^{13}\text{C}_{\text{CO}_2} -11\text{‰}$ to $\delta^{18}\text{O}_{\text{H}_2\text{O}} -1\text{‰}$ and $\delta^{13}\text{C}_{\text{CO}_2} -3\text{‰}$.

The isotopic composition of main- and late-stage calcite were mostly different from one another, but some late-stage values overlapped with main-stage calcite (Figure 5F). The main-stage data were more varied in $\delta^{18}\text{O}_{\text{H}_2\text{O}}$, whereas the range of late-stage $\delta^{13}\text{C}_{\text{CO}_2}$ ex-

tended to larger negative values. Careful evaluation of values in the overlap demonstrated that they are not a result of misclassification of main-stage calcite as late-stage or simply analytical-temperature errors [18].

6. Discussion

Based on geologic reasoning and inferences, there have been multiple proposed sources of the main-stage hydrothermal fluids over the past century. Several of the possible sources of hydrothermal fluids are constrained, whereas some are not. We first review the currently accepted model of the main-stage hydrothermal system followed by an evaluation of the most likely sources of the main-stage hydrothermal fluid in light of the carbon and oxygen isotope composition of the hydrothermal fluids as calculated from main-stage calcite.

The source of late-stage hydrothermal fluids has only been briefly considered in the published literature. We evaluate the sources of late-stage hydrothermal fluids with our limited oxygen and carbon isotope compositions of the late-stage hydrothermal fluids as calculated from late-stage calcite.

6.1. Review of Main-Stage Hydrothermal System

Since about 1970 it has been widely accepted that native copper ore-forming hydrothermal fluids were generated by burial metamorphism [5]. Mineralogic, stable isotope, and fluid inclusion studies by Livnat [6] and Püschner [7] supported the hypothesis that the ore-forming fluids were dominantly of metamorphic origin. Interpretation of unimodal normally distributed copper isotope composition of hydrothermally precipitated native copper also supports a metamorphic-dominated origin of the ore-forming fluids ([29,44]). The correspondence of the timing of native copper deposition and peak temperatures at depth [45] is consistent with burial metamorphism. The widespread distribution of anomalous amounts of copper in exposed basalt-dominated strata throughout the rift (Figure 1) is indicative of a large-scale regional hydrothermal event easily explained by burial metamorphic processes. The district-scale regular mineral zones (Figure 2) fit well with regional burial metamorphogenic-hydrothermal processes, wherein fluids are focused within the native copper district. The most likely source of most of the copper is from leaching of the rift-filling basalt-dominated volcanic rocks, including from the PLV host rocks, from a zone down-dip and at depth beneath the native copper deposits at temperatures between 300 to 500 °C (Figure 3) [5,29,45].

The almost exclusive precipitation of native copper during the main-stage hydrothermal event places a significant constraint on the source of hydrothermal fluids. There was a lack of sulfur in the entire hydrothermal system from the rocks in the source zone to the rocks of the pathways of ascending ore-forming fluids and to the PLV host rocks in the zone of precipitation (Figure 3B) [5]. The lack of sulfur resulted in native copper instead of copper sulfides. This lack of sulfur can be explained by a low sulfur magma [29,44] that loses sulfur by degassing of sulfur from the subaerial volcanic rocks prior to solidification [5,46].

The lack of sulfur in the main-stage hydrothermal ore-forming system was used as an argument against involvement of magmatic fluids, and in support of metamorphic fluids, as elsewhere magmatic fluids typically result in sulfide-bearing hydrothermal minerals [5]. The age of the regional hydrothermal event at about 1070 to 1040 Ma [30–32] is more than 15 to 30 million years after emplacement of abundant basalt-dominated volcanic rocks of the Midcontinent Rift which generally ended about 1085 Ma [47]; the youngest exposed igneous body in the Midcontinent Rift is about 1075 Ma (Bear Lake igneous body within the Freda Sandstone (Figure 2) [25]. The age gap between known igneous activity and the hydrothermal event suggests that magmatic fluids were not a significant contributor to the ore-forming fluids, and any contribution would have more likely come from the waning stage of deep crystallizing magma bodies such as in the upper mantle or lower crust. Livnat's [6] interpretation of his light stable isotope data did not acknowledge any component of magmatic fluids, while Püschner's [7] interpretation of his stable isotope

data led him to conclude that although a contribution of magmatic fluids to the ore-forming fluid was not indicated, neither could a magmatic fluid contribution be excluded.

Jolly [8] demonstrated that ore-forming hydrothermal fluids were likely at least moderately saline. Püschner and Kelly [7,48] documented high salinity ore-forming fluids using fluid inclusion studies. Brown [49,50] reasoned that moderate to high salinity of the ore-forming fluids was an essential component of the ore-forming fluids and that metamorphic processes were not likely capable of generating high enough salinity. Thus, the ore-forming fluids could not be composed of only metamorphic fluids, as an outside source of salinity was required.

Brown [49,50] proposed that downward-moving hydrodynamically evolved formation water with a meteoric source entered the source zone and contributed salinity and copper to the metamorphic-dominated processes generating the ore-forming fluids. In Brown's [49,50] model, meteoric water begins at shallow depths in the rift-filling clastic sedimentary rocks overlying the PLV and overlying the source zone (Figure 3B). This meteoric water spends considerable time reacting with and evolving in these sedimentary rocks, gaining salinity by dissolving evaporitic minerals from postulated evaporite horizons and from cement as the water moved downward and into the source zone. Brown [49,50] proposed that a highland area on the Isle Royale limb of the rift (Figure 3B) led to gravity-driven meteoric water flow. Brown's [49,50] proposed hydrodynamic evolved formation waters with a meteoric source are analogous to volumetrically abundant evolved meteoric water in major sedimentary basins, well recognized for their role in mineral deposits [51]. Brown's model [49,50] does not satisfy the constraint of very low to no sulfur in the ore-forming fluids as he did not provide a mechanism to deplete sulfur that was very likely acquired from dissolution of evaporitic minerals. In addition, the copper isotope signature of native copper is not consistent with a significant amount of copper in the hydrodynamic evolved meteoric water leached from the clastic sedimentary rocks unless it was overwhelmed by metamorphogenic-derived copper. Bornhorst and Mathur [29,44] also argue that the more complex nature of a hydrodynamic model is less consistent with the observed limited copper isotopic variability. Thus, it seems unlikely that hydrodynamic evolved meteoric water was the principal outside source of salinity, but a limited contribution cannot be precluded.

If Brown's [49,50] salinity constraint is correct, Bornhorst [52] hypothesized that evolved formation water with a seawater source is a reasonable source of salinity in the ore-forming fluids. Modern midocean ridge vent systems expel evolved seawater hydrothermal fluids that are very low or devoid in sulfur [53,54]. Sulfur-bearing seawater is heated as it moves downward through tholeiitic basalt and at about 130 to 150 °C anhydrite begins to precipitate, which removes sulfur from the evolving seawater. There is likely insufficient available Ca in the fluids to completely remove all of the sulfur. Albitization of the basalt, beginning at about 250 °C, provides abundant Ca to the hydrothermal fluid, which is more than enough for additional precipitation of anhydrite to remove all of the sulfur from the fluids leaving an excess of Ca from derived by albitization. This excess results in Ca-rich brines that are characteristic of burial metamorphism of basalts in continental rift systems [55]. The ore-forming fluids of the Keweenaw Peninsula are likely Ca-rich brines [6,48]. This mechanism to deplete sulfur from evolved seawater allows closed to open system formation water (seawater) to be a viable source of salinity in the ore-forming fluids (Figure 3C). Even less depletion of sulfur is needed for Mesoproterozoic seawater as compared to modern seawater because Mesoproterozoic seawater is notable for being comparatively low in sulfur [56].

Precipitation of native copper and associated main-stage minerals is hypothesized to be the result of cooling of the fluids and reaction of the fluids with host rocks [8,29]. Bornhorst and Woodruff [10] hypothesized that in addition to these two mechanisms, mixing of ore forming fluids with copper-poor and sulfur-poor shallow reduced meteoric waters played a role in precipitation, although their evidence was not conclusive. The initial object of this research was to test this hypothesis with new oxygen and carbon stable isotope data.

6.2. Main-Stage Hydrothermal Fluid Oxygen Isotope Composition

The $\delta^{18}\text{O}_{\text{H}_2\text{O}}$ values were mostly within the range for metamorphic waters proposed by Sharp [51] (Figure 7). Only three samples fell below -3‰ . Values of $\delta^{18}\text{O}_{\text{H}_2\text{O}}$ greater than $+10\text{‰}$ were within the $\delta^{18}\text{O}_{\text{H}_2\text{O}}$ range for only metamorphic waters; these represent $\sim 30\%$ of the measured values. While it is possible to explain the $\delta^{18}\text{O}_{\text{H}_2\text{O}}$ as almost exclusively of metamorphic origin, the standard metamorphic range is large enough to encompass the wide variety of world-wide metamorphic protoliths and variable conditions. Thus, such a range is not necessarily applicable to a single geologic setting.

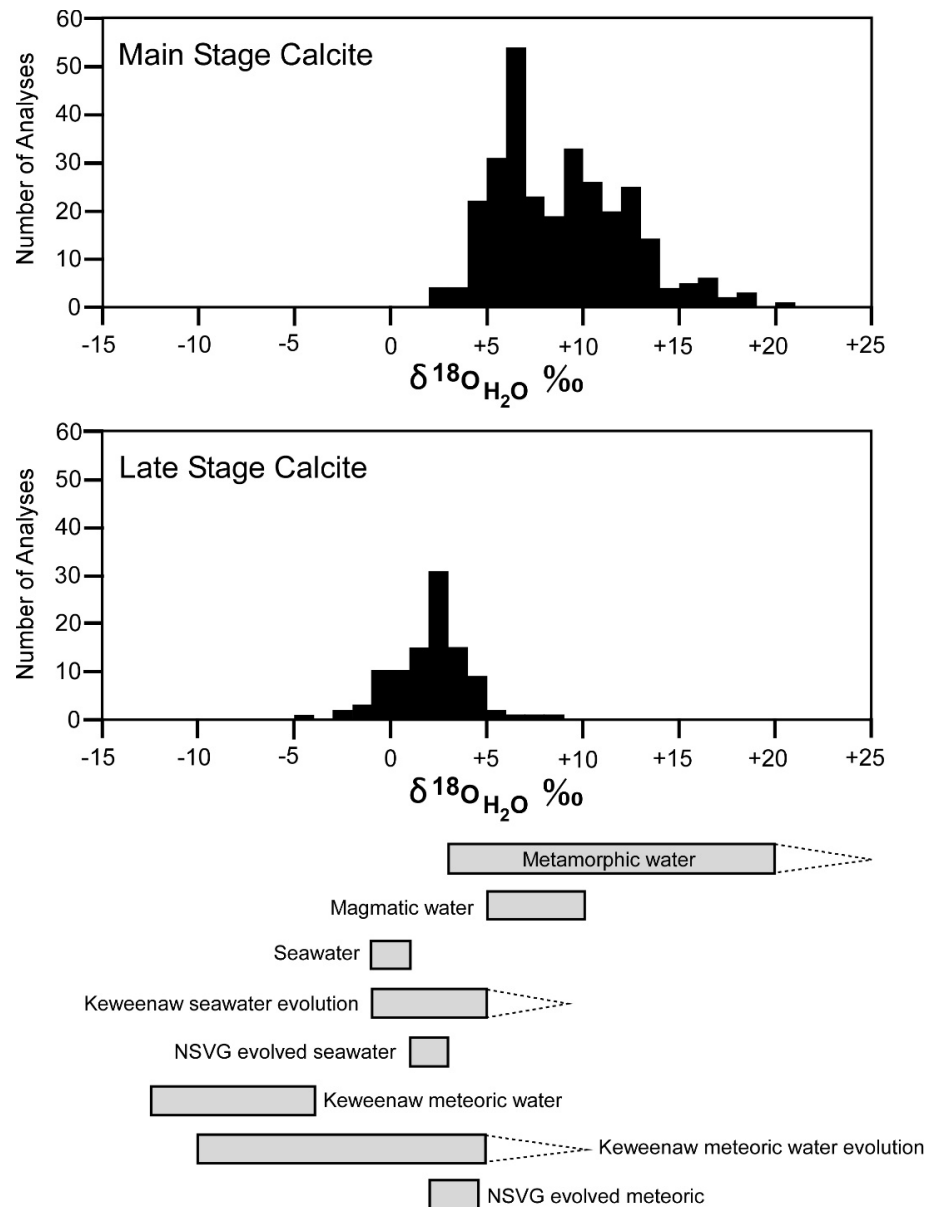


Figure 7. Histogram of oxygen isotopic composition of calcite from the Keweenaw Peninsula native copper district. Oxygen isotopic composition of various types of water given below in shaded boxes with open area denoting possible higher values. Metamorphic water [51,57], magmatic [15], seawater [51], Keweenaw seawater evolution [51,58], North Shore Volcanic Group (NSVG) evolved seawater [58], Keweenaw meteoric water [6,58], Keweenaw meteoric water evolution [6,51,58], and North Shore Volcanic Group (NSVG) [58]. Analytical and temperature uncertainty is shown in Figure 5. Temperature uncertainty is discussed in Sections 4.3 and 6.5.

The isotopic composition of metamorphic waters depends on factors such as cumulative or bulk $\delta^{18}\text{O}$ composition of the protolith, temperature, fluid-to-rock ratio, fractionation between the rock and fluid, fraction of element remaining, and batch (closed system) versus Rayleigh (open system) fractionation [51,59]. Metamorphic fluids with high $\delta^{18}\text{O}_{\text{H}_2\text{O}}$, tend to be from metamorphosed sedimentary rocks with pre-metamorphic elevated $\delta^{18}\text{O}$. Metamorphic dehydration reactions typically result in a shift in whole-rock values of less than a few per mil and more commonly less than 1‰ [51]. Thus, the isotopic composition of metamorphic fluids, for a first approximation, can be assumed to be similar to the pre-metamorphic bulk rock isotopic composition.

The thick rift-filling section within the source zone (Figure 3) is basalt-dominated with interbedded rhyolite and volcanoclastic sedimentary layers. Livnat [6] found that the least altered massive flow interiors of basalt lava flows of the rift-filling PLV have whole-rock $\delta^{18}\text{O}$ typically between +7‰ to +8‰ and up to +10‰. These interiors of flows were likely $\delta^{18}\text{O}$ enriched by pre-metamorphic processes [6]. Park and Ripley [58] found that 80% of the whole rock $\delta^{18}\text{O}$ from the massive interiors of basalt lava flows from the North Shore Volcanic Group (NSVG), stratigraphically slightly older than the PLV, to be less than +10‰ and values of least altered NSVG volcanic and hypabyssal rocks to be in the +5‰ to +8‰. The rift-filling rhyolitic rocks in the PLV have elevated whole-rock $\delta^{18}\text{O}$ between +12‰ to +16‰ enriched by pre-metamorphic processes [6]. In addition to the volcanic rocks, volumetrically minor, immature, volcanoclastic conglomerate and sandstone are interbedded with exposed rift-filling volcanic rocks. These volcanoclastic sedimentary rocks are composed of clasts of mostly rhyolite with lesser basalt and are expected to have pre-metamorphic whole-rock $\delta^{18}\text{O}$ elevated above values for basalt or rhyolitic rocks because of limited ^{18}O -rich weathering products and pre-metamorphic meteoric water alteration. The volcanoclastic whole-rock $\delta^{18}\text{O}$ is likely between about +10‰ to +20‰. The proportion of the source zone rocks is not well defined, in large part because of a large amount of buried stratigraphic section. As the hydrologic pathways change over time during metamorphism, it is reasonable to expect that individual batches of metamorphic fluid could be derived from a restricted volume of rocks of lesser abundance. Thus, the possible range in the isotopic composition of batches of fluids derived by metamorphic processes could be from between +5‰ to +20‰, or perhaps slightly higher. We estimate that the most common $\delta^{18}\text{O}_{\text{H}_2\text{O}}$ of a batch of fluid derived by metamorphic processes is about +7‰ to +13‰. By this reasoning, it is possible to explain most of the $\delta^{18}\text{O}_{\text{H}_2\text{O}}$ values as simply derived by metamorphic processes, with the higher values representing batches of fluid derived from restricted volumes of rock. However, in addition to the three $\delta^{18}\text{O}_{\text{H}_2\text{O}}$ values of +3‰ or less, there are an additional 26 values of +5‰ or less, for a total of 29 values or 10% of the values that are not easily explained by metamorphic processes alone. Those values between +5‰ to +7‰ are less easily explained by metamorphic processes alone, as they are below the predicted most common values of the metamorphogenic-hydrothermal fluid. We interpret that all $\delta^{18}\text{O}_{\text{H}_2\text{O}}$ values of +7‰ or less, or a total of 116 values (40% of the data), are readily explained by mixing between a metamorphic-derived fluid and an additional fluid. To explain all of the lower $\delta^{18}\text{O}_{\text{H}_2\text{O}}$ values of the hydrothermal fluids, the oxygen isotope composition of this added fluid was less than about +2‰.

The oxygen isotope data are consistent with metamorphic processes dominating the ore-forming hydrothermal fluids; however, we conclude that metamorphic processes alone are not responsible for the entirety of the large variation in oxygen isotopic composition of the hydrothermal fluids (Figure 7). An additional type of fluid was likely involved in the hydrothermal system.

6.3. Main-Stage Hydrothermal Fluid Oxygen and Carbon Isotope Co-Variation

The carbon isotope composition of the hydrothermal fluids when combined with the oxygen isotope composition provides an additional constraint on the sources of waters in the hydrothermal system, although the carbon isotope fingerprint of the source of waters

is less clear. The predicted conditions of ore-forming fluid [6,8] indicate that calculated $\delta^{13}\text{C}_{\text{CO}_2}$ is approximately $\delta^{13}\text{C}_{\Sigma\text{C}}$ of the fluids [43].

Most of the $\delta^{13}\text{C}_{\text{CO}_2}$ values calculated for the hydrothermal fluids fell within a band between -2‰ to $+2\text{‰}$, with the highest concentration between -1‰ to $+1\text{‰}$, with variable $\delta^{18}\text{O}_{\text{H}_2\text{O}}$ (Figures 5E and 8). The band is approximately in the middle of the carbon isotope range for marble and marine limestone and is above the carbon isotope range of magmatic CO_2 with only few values falling within the magmatic range (Figure 8). The $\delta^{13}\text{C}_{\text{CO}_2}$ values fell within the carbon isotope range for freshwater limestone.

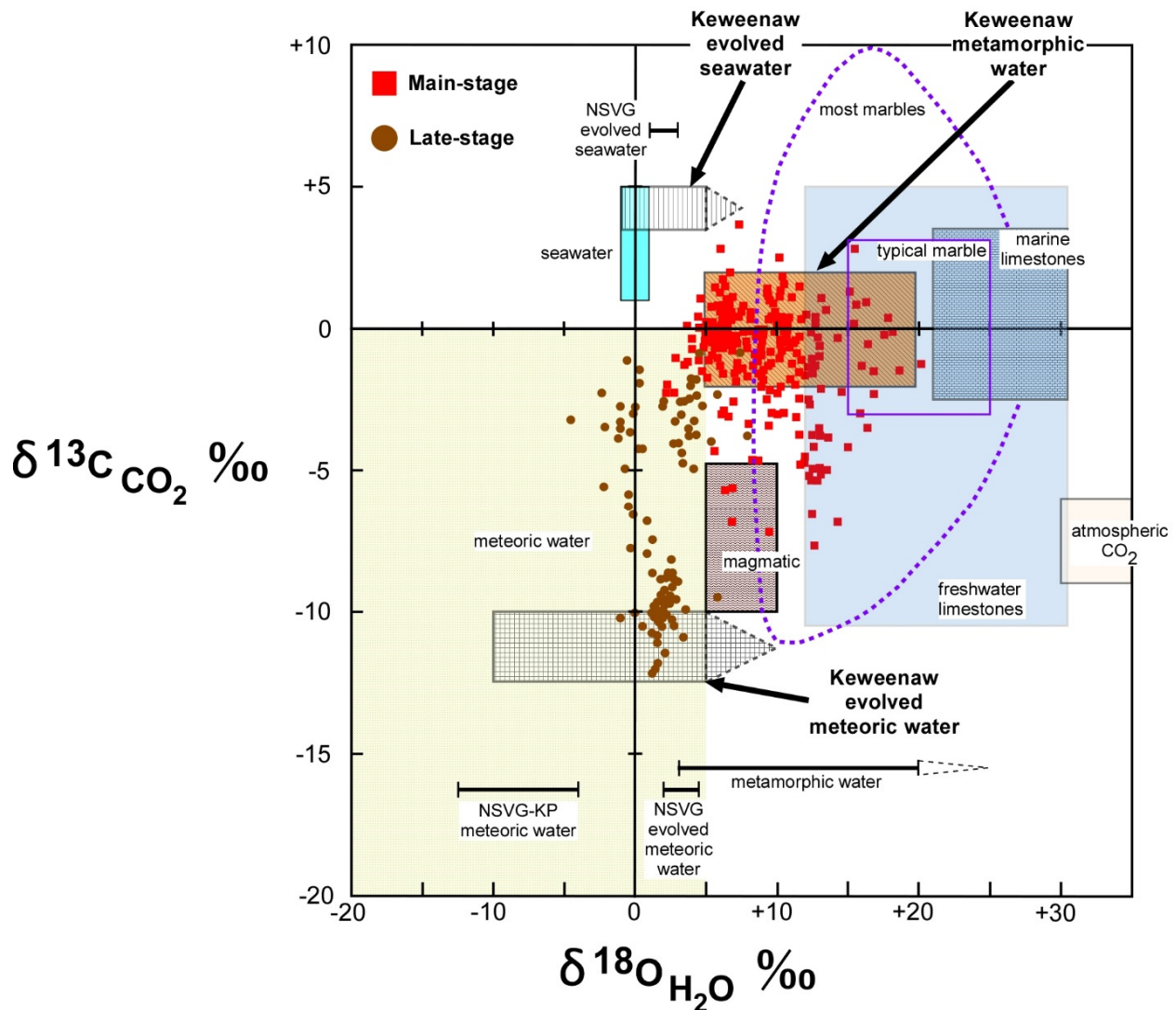


Figure 8. Interpretative carbon and oxygen isotopic co-variation of calcite from the Keweenaw Peninsula native copper district. Patterned boxes are proposed carbon and oxygen isotopic composition of Keweenaw metamorphic water, Keweenaw evolved seawater, and Keweenaw evolved meteoric water involved in the Keweenaw Peninsula native copper district. Only oxygen isotopic range for NSVG (North Shore Volcanic Group water involved in low grade metamorphic alteration from Park and Ripley [58], oxygen isotopic range for NSVG (North Shore Volcanic Group-Keweenaw Peninsula meteoric water from Park and Ripley and Livnat [6,58], and range of oxygen isotopic composition of metamorphic water from [51,57]; carbon arbitrarily plotted. Fields for carbon and oxygen isotopic composition of seawater, magmatic, typical marble (dotted outline), marine limestones, most marbles, freshwater limestones, and atmospheric CO_2 from Sharp [51]. Analytical and temperature uncertainty shown in Figure 5. Temperature uncertainty discussed in Sections 4.3 and 6.5.

Like oxygen, the carbon isotope composition of hydrothermal fluids derived via metamorphism depends on several factors, especially the bulk $\delta^{13}\text{C}$ composition of the protolith and, similarly, the metamorphic derived CO_2 is expected to have about the same isotopic composition as the protolith being metamorphosed. The source area igneous rocks are expected to have a low abundance of carbon with magmatic $\delta^{13}\text{C}$ of -10% to -4% . We expect the abundance of magmatic carbon in the rift-filling basalt-dominated source rocks will be overwhelmed by post-emplacment pre-metamorphic added carbon. Pre-metamorphic carbon is also likely the dominant source of carbon in the interbedded red-colored volcanoclastic sedimentary rocks. The climatic setting of the Midcontinent Rift was arid to semi-arid [19,23] and such climates are well known for the formation of widespread caliche. In continental arid and semi-arid regions caliche is an important sink of carbon [60]. The similarity of $\delta^{13}\text{C}$ in carbonates since the Mesoproterozoic suggests that modern oceanic and atmospheric carbon isotopic values are generally representative of the Mesoproterozoic. Caliche influenced calcite cement has been documented in interbedded volcanoclastic sedimentary rocks within PLV as well as the overlying clastic sedimentary rocks of the Copper Harbor Formation [19,61]. Caliche forms in the tops of subaerial basalt lava flows and along fractures. Caliche on young basalt in Arizona, USA has a $\delta^{13}\text{C}$ of between -7% to $+14\%$, midpoint of about $+3.5\%$, as compared to atmospheric CO_2 $\delta^{13}\text{C}$ of -7% [62]. Calcite cement and caliche precipitated from water in equilibrium with an atmospheric CO_2 of -7% , has a $\delta^{13}\text{C}$ of about $+3\%$ at 25°C . Evaporation resulting in residual waters that then precipitate calcite results in elevated $\delta^{13}\text{C}$ above $+3\%$. The $\delta^{13}\text{C}$ values of freshwater limestones of between -11% to $+5\%$ and marine limestones between -4% to $+4\%$ (Figure 8) provide an additional guide to values for diagenetic carbonate as both meteoric water and seawater could have been present in pore spaces given a non-marine and/or marine environmental setting, which was likely present during deposition of the younger PLV and interbedded volcanoclastic sedimentary rocks. Livnat [6] determined $\delta^{13}\text{C}$ of -1.6 to -4.6% for several calcite samples from the overlying Copper Harbor Formation, which are lithologically and environmentally similar to interbedded volcanoclastic sedimentary rocks within the PLV. He classified these samples as calcite cement; however, the origin of this carbonate is uncertain. The range in comparative carbon isotopic composition of pre-metamorphic calcite is large, we estimate possible range in bulk whole-rock $\delta^{13}\text{C}$ could be from -4% to $+4\%$ and more likely -2% to $+2\%$, and perhaps within an even smaller range. This bulk whole-rock $\delta^{13}\text{C}$ is capable of yielding fluids with metamorphic $\delta^{13}\text{C}_{\text{CO}_2}$ that matches the most common carbon isotopic compositions of the hydrothermal fluids from -2% to $+2\%$ and shown as Keweenaw metamorphic water in Figure 8. Carbon isotope values on both the high and low sides of the most common values may not be the result of metamorphic processes alone.

The oxygen and carbon isotope data are consistent with metamorphic processes dominating the ore-forming hydrothermal fluids. The higher carbon isotope values, above the probable metamorphic range of $\delta^{13}\text{C}_{\text{CO}_2}$ -2% to $+2\%$ were few (four values) and can be readily explained by addition of a fluid with $\delta^{13}\text{C}_{\text{CO}_2}$ of $+4\%$ or greater (slightly above the highest value). The oxygen isotope composition of this added fluid is not constrained but is likely within the range of observed values.

There was a total of 61 $\delta^{13}\text{C}_{\text{CO}_2}$ values (23%) with -2% or less that were not easily explained simply by metamorphic processes. Of these values, 22 (8%) have $\delta^{13}\text{C}_{\text{CO}_2}$ values with -4% or less and are more difficult to explain by metamorphic processes alone. These lowest $\delta^{13}\text{C}_{\text{CO}_2}$ values had corresponding $\delta^{18}\text{O}_{\text{H}_2\text{O}}$ between about $+5\%$ to $+15\%$ (Figure 8). The outer envelope of the lower $\delta^{13}\text{C}_{\text{CO}_2}$ values converges on $\delta^{13}\text{C}_{\text{CO}_2}$ about -10% and $\delta^{18}\text{O}_{\text{H}_2\text{O}}$ about $+10\%$. Mixing of a fluid with $\delta^{13}\text{C}_{\text{CO}_2}$ of -10% or less could readily explain the lower values as well as $\delta^{13}\text{C}_{\text{CO}_2}$ values between -2% and -4% . The oxygen isotope composition of this added fluid is not constrained, but the lowest carbon isotope values suggest the oxygen isotope composition could be within or near the range of measured values.

6.4. Main-Stage Hydrothermal Fluids

A significant amount of the oxygen and carbon isotopic data can be explained by metamorphic fluids alone. However, a significant number of samples are outside of the probable range for metamorphic processes and are not easily explained by metamorphic processes alone. In addition, the low isotopic contrast between metamorphic fluids and likely additional fluids, and the relatively wide range of isotopic composition of metamorphic fluids alone, are permissive of the ore-forming fluids being dominated by metamorphic fluids but also containing a significant amount of other fluids. As described above, the absolute values and heterogeneity of the data are best interpreted to have been the result of mixing of the metamorphic waters with at least two additional waters at two different depths. The carbon isotopes suggest that one of these waters had $\delta^{13}\text{C}_{\text{CO}_2}$ of +4‰ or greater to explain the highest $\delta^{13}\text{C}_{\text{CO}_2}$ values, and the other had $\delta^{13}\text{C}_{\text{CO}_2}$ of −10‰ or less to explain the lower values. At least one of these fluids had $\delta^{18}\text{O}_{\text{H}_2\text{O}}$ +2‰ or less to explain the lowest $\delta^{18}\text{O}_{\text{H}_2\text{O}}$ fluids.

There are several candidates for the source of the additional waters. Based on only $\delta^{18}\text{O}_{\text{H}_2\text{O}}$, the likely candidates are (a) seawater or evolved seawater; (b) meteoric water, and/or evolved meteoric water; and/or magmatic water (Figure 7). The simplest choice for the source of the additional fluid with $\delta^{13}\text{C}_{\text{CO}_2}$ of +4‰ or greater is seawater or evolved seawater (Figure 8). Given the bulk carbon isotopic composition of the source zone, it seems less likely that evolved meteoric water could have reached $\delta^{13}\text{C}_{\text{CO}_2}$ of +4‰ or greater, a value greater than the bulk composition of the source zone. We have estimated the bulk composition of the clastic sedimentary rocks overlying the source zone in which Brown's [49,50] proposed meteoric waters hydrodynamically evolved (Figure 5B). Compared to the bulk composition, the hydrodynamic evolution of meteoric water in the overlying clastic sedimentary rocks is unlikely to have reached high enough $\delta^{13}\text{C}_{\text{CO}_2}$. Evolved seawater could have had high enough $\delta^{13}\text{C}_{\text{CO}_2}$ and low enough $\delta^{18}\text{O}_{\text{H}_2\text{O}}$ (+2‰ or less) to explain both the high $\delta^{13}\text{C}_{\text{CO}_2}$ and low $\delta^{18}\text{O}_{\text{H}_2\text{O}}$ of the hydrothermal fluids. We propose that evolved formation water with a seawater source mixed with metamorphic-dominated fluids. The mixing of metamorphic fluids with evolved seawater not only explains some of the isotopic variation, it also provides an outside source of salinity for the ore-forming fluids, a critical constraint, as proposed by Brown [49,50]. Given the low isotopic contrast, it is permissible that even those samples readily explained by metamorphic fluids alone could have a significant amount of evolved seawater.

Low grade metamorphic/hydrothermal alteration of the NSVG formed within the same time interval as the metamorphic/hydrothermal fluid minerals of the Keweenaw Peninsula [31,36]. Using oxygen and limited hydrogen isotope data, Park and Ripley [58] proposed that the alteration of the NSVG formed from fluids that were a mixture of evolved seawater and evolved meteoric water but lacked a metamorphic water component. The NSVG model supports involvement of evolved seawater in the metamorphic/hydrothermal system of the Keweenaw Peninsula. Additionally, Livnat [6] proposed seawater played an important role in the hydrothermal fluids based on limited isotopic evidence. However, Püschner [7] reported that his calculations suggest a seawater component in the hydrothermal system was unlikely.

The second added fluid must have a $\delta^{13}\text{C}_{\text{CO}_2}$ of about −10‰ or less, but the oxygen isotopic composition is not well constrained. The likely candidates are (a) meteoric water or evolved meteoric water, or (b) magmatic water (Figure 8). Based on oxygen-hydrogen isotopic paired data from low grade metamorphic alteration minerals in the NSVG, Park and Ripley [58] proposed that meteoric waters had $\delta^{18}\text{O}_{\text{H}_2\text{O}}$ between about −10‰ to −12.5‰ and evolved to a $\delta^{18}\text{O}_{\text{H}_2\text{O}}$ of +2‰ to +4.5‰. Their NSVG evolved meteoric water mixed with evolved seawater. This evolved meteoric water, with a range of $\delta^{18}\text{O}_{\text{H}_2\text{O}}$ of +2‰ to +4.5‰, could have had low enough $\delta^{13}\text{C}_{\text{CO}_2}$, such as −10‰ to −15‰, to be able to explain the $\delta^{18}\text{O}_{\text{H}_2\text{O}}$ and $\delta^{13}\text{C}_{\text{CO}_2}$ variation in the Keweenaw hydrothermal fluids. The magnitude of $\delta^{18}\text{O}_{\text{H}_2\text{O}}$ evolution of meteoric water as proposed by Park and Ripley [58] is less than that observed for formation waters with a meteoric source from elsewhere; where evolution in $\delta^{18}\text{O}_{\text{H}_2\text{O}}$ can be from about −14‰ up to +10‰, as was documented

by Sharp [51]. The geologic arguments presented above suggest that magmatic water was not a significant component of the hydrothermal fluids and is discussed further in the next section. Therefore, we propose that evolved meteoric water was a component of the hydrothermal fluid. The low $\delta^{13}\text{C}_{\text{CO}_2}$ composition of this evolved meteoric water suggests that it was reducing and would have to have been very low in sulfur and likely also low in copper.

6.5. Depth of Fluid Mixing of Main-Stage Hydrothermal Fluids

The ore-forming fluid was generated at depth in a source zone below the native copper deposits by metamorphic dominated processes (Figure 3). This metamorphic fluid mixed with evolved seawater and evolved meteoric water prior to precipitation of main-stage minerals, including native copper. Mixing of metamorphic fluids with additional isotopically different fluids could have occurred at two end-member depths: in the deep source zone undergoing metamorphism with the additional fluid participating in generating the ore-forming fluid, or in the relatively shallow zone of precipitation with the additional fluid participating in reduction of copper from the fluid to precipitate native copper (Figure 5C).

One of our proposed additional fluids is evolved seawater. Brown [49,50] suggested that an outside source of salinity was needed during generation of the ore-forming fluid by metamorphic processes. Evolved seawater added into the deep source zone would have provided salinity in the source zone and thereby participated with burial metamorphic waters to produce a hybrid ore-forming fluid. At depth in the source zone, we expect the isotopically evolved seawater that is added to the metamorphic fluid would become relatively well mixed resulting in a batch of hybrid ore-forming fluid with a more or less homogeneous isotopic composition. Since the difference in the oxygen and carbon isotopic composition between the metamorphic fluid and evolved seawater is small, even a modest to significant proportion of evolved seawater in a well-mixed hybrid may not result in a recognizable isotopic shift from a metamorphic fluid alone. Thus, a significant proportion of evolved seawater in the hybrid ore-forming fluid is, therefore, permissible.

In contrast to the deep source zone, we expect that the degree of mixing between a hybrid ore-forming and an evolved meteoric water in the zone of precipitation would range from poor to well. Shallow mixing would have a much higher degree of isotopic heterogeneity depending on the isotopic contrast between the waters being mixed. In addition, there is likely a temperature contrast between deep and shallow fluids with the deep sourced fluids being hotter. The consistency of the mineral zones suggests that mixing of the deep and shallow fluids was generally good and resulted in a more or less consistent temperature, resulting in consistent mineral zones. Thus, we expect that the temperature variation within the zone of precipitation due to mixing of fluids with different temperatures to be within the uncertainty of temperature within the zones themselves, as discussed in Section 4.3. The temperature uncertainty can only explain a limited amount of the isotopic variability.

The isotopic composition of the proposed Keweenaw evolved meteoric water is much different than the metamorphic waters or hybrid ore-forming fluid. The spot oxygen and carbon values determined by SIMS document a high degree of within-sample isotopic variation with variation of roughly at least plus or minus 1‰ to 3‰ for both $\delta^{18}\text{O}_{\text{H}_2\text{O}}$ and $\delta^{13}\text{C}_{\text{CO}_2}$. This 2‰ variation relative to the median for each (2‰ divided by absolute value of the median) is 24% for oxygen and 360% for carbon. The carbon isotopic data are relatively much more variable than the oxygen isotopic data. There was a high degree of within-sample $\delta^{18}\text{O}_{\text{H}_2\text{O}}$ and especially $\delta^{13}\text{C}_{\text{CO}_2}$ variation at the sub-mm to cm scale within a single continuous mass of calcite showing growth rings (Figure 6). This small-scale variation is especially difficult to ascribe to compositional variation from well-mixed deep processes. The simplest explanation of the high degree of within-sample variation is shallow mixing of evolved meteoric water in the zone of precipitation. The especially high variability in carbon isotope composition of the hydrothermal fluids (Figure 8) is

illuminated by SIMS data (Figures 5D and 6) and is apparently averaged away in the bulk data.

The oxygen and carbon isotopic characteristics of magmatic fluids suggest that they potentially could have been mixed with the ore-forming fluids instead of evolved meteoric water (Figure 8). However, the age range of rift magmatism suggests that if magmatic fluids were a component of the hydrothermal system, it is more likely that such fluids were contributed from deep magma bodies below the source zone during the waning stages of crystallization. Thus, magmatic fluids would have been part of the deep processes where well-mixed metamorphic water and evolved seawater resulted in a hybrid ore-forming fluid. Given the size of the metamorphogenic-hydrothermal system, it is unlikely that magmatic fluids could have made it to shallow depths of the zone of precipitation without becoming part of the hybrid ore-forming fluid. The isotopic data cannot conclusively preclude magmatic fluids as a minor component of hybrid ore-forming fluids as previously concluded by Püschner [7].

6.6. Late-Stage Fluids

The oxygen and carbon isotopic composition of late-stage calcite was generally different from main-stage calcite (Figure 5F). There was a bimodal distribution of late-stage carbon and oxygen isotope values less than $\delta^{13}\text{C}_{\text{CO}_2} \sim -5\text{‰}$ with one group of values overlapping the field of main-stage values and the other being a linear trend with variable carbon from $\delta^{13}\text{C}_{\text{CO}_2} -12\text{‰}$ to -1‰ and approximately constant $\delta^{18}\text{O}_{\text{H}_2\text{O}}$ centered around $\sim 0\text{‰} \pm 4\text{‰}$ (Figure 8). Similar to main-stage fluids, the temperature uncertainty can only explain a limited amount of the isotopic variability.

The overlap between the late-stage and main-stage hydrothermal fluid isotopic compositions suggests they both involve at least one common fluid, likely the hybrid metamorphic-dominated ore-forming fluids (Figure 8). The two groups of calculated $\delta^{13}\text{C}_{\text{CO}_2}$ occur within sample WAS-121 (see Section 5.3). The cathodoluminescence image of WAS-121 (see Supplementary Materials) indicates that the group overlapping the field of main-stage values was precipitated before the linear trend; there were at least two pulses of late-stage hydrothermal fluids. Given the low frequency of late-stage hydrothermal fluid oxygen and carbon isotopic values falling within the overlap area, it seems likely that ore-forming fluids were a lesser component in the late-stage hydrothermal fluids. The occurrence of ore-forming hydrothermal fluids in both the main-stage and late-stage hydrothermal event is consistent with the main-stage and late-stage hydrothermal events being continuous with one another.

The linear trend of values is suggestive of mixing of two fluids with different $\delta^{13}\text{C}_{\text{CO}_2}$. The likely candidates of these two fluids are either two different meteoric waters or seawater and meteoric water (Figure 8). The late-stage fluid with $\delta^{13}\text{C}_{\text{CO}_2} \sim -1\text{‰}$ or greater and $\delta^{18}\text{O}_{\text{H}_2\text{O}} \sim 0\text{‰}$ could be either seawater or meteoric water, likely shallow evolved seawater. It is unlikely that this fluid is of the same origin as the main-stage evolved sulfur-depleted seawater contributed at depth into the source zone. The relatively low temperatures of precipitation of the late-stage minerals are consistent with the evolution of late-stage seawater in the relatively shallow environment near the depth of the zone of precipitation. In this environment evolved seawater would not necessarily become depleted in sulfur. Since the late-stage fluids are associated with the precipitation of copper sulfides, one of them had a significant amount of sulfur. A late-stage hydrothermal fluid containing shallow evolved seawater with sulfur could have provided the needed late-stage source of sulfur. Alternatively, a late-stage fluid with these isotopic characteristics could have been evolved meteoric water containing sulfur instead of shallow evolved seawater.

The late-stage fluid with $\delta^{13}\text{C}_{\text{CO}_2} \sim -14\text{‰}$ or less and $\delta^{18}\text{O}_{\text{H}_2\text{O}} \sim 0\text{‰}$ is likely an evolved meteoric water. This fluid is isotopically similar to the main-stage evolved meteoric water mixed with hybrid ore-forming fluid in the zone of precipitation. If this late-stage fluid is of the same origin as the main-stage evolved meteoric fluid, then it is likely very low or devoid in sulfur requiring the other late-stage fluid to be sulfur-bearing, as described

above. Alternatively, this fluid could have been sulfur-bearing consistent with a reducing characteristic indicated by the low $\delta^{13}\text{C}_{\text{CO}_2}$. This late-stage evolved meteoric water is similar in $\delta^{18}\text{O}$ to the evolved meteoric water component proposed by Park and Ripley [58] for the NSVG (Figure 8).

The oxygen and carbon isotopic composition of late-stage hydrothermal fluids suggests that they were likely the result of mixing of three different fluids. A minor component of the late-stage hydrothermal fluids was hybrid metamorphic-dominated ore-forming fluids. The late-stage hydrothermal fluids were dominated by either two types of evolved meteoric waters or evolved meteoric water and seawater. In contrast to the main-stage hydrothermal fluids, at least one of the sources of the late-stage hydrothermal fluids was sulfur-bearing as they precipitated copper sulfides. We favor the hypothesis that the late-stage hydrothermal fluids were dominated by a mix of evolved meteoric water, of similar composition as main-stage meteoric water with shallow evolved seawater and main-stage hybrid metamorphic-dominated native copper ore-forming fluid.

The Paleoproterozoic rocks underlying the edges of the Mid-continent rift contain scattered pyrite in marine deposited sedimentary rocks, metamorphosed before Keweenaw time, and could have been saturated in seawater. As the main-stage ore-forming hydrothermal system collapsed, it is a reasonable hypothesis that seawater from within these rocks could have become a part of the late-stage hydrothermal system, providing a source of sulfur.

7. Conclusions

The Mesoproterozoic Midcontinent rift-filling rocks exposed on the Keweenaw Peninsula were altered during an extensive regional hydrothermal event (Figure 3). This hydrothermal event resulted in the Keweenaw Peninsula native copper district. The minerals of this event can be temporally subdivided into those precipitated during the main-stage of hydrothermal activity coincident with native copper deposition and a superimposed late-stage. Spatial zoning of main-stage low grade metamorphogenic-hydrothermal mineral assemblages, documented herein, demonstrate that a thermal high is associated with the native copper deposits. The district-wide late-stage low temperature mineral assemblage is not spatially zoned.

1. For more than five decades, the main-stage hydrothermal event has been interpreted to have been the result of burial metamorphism. The main-stage, sulfur-poor, ore-forming fluids are confirmed to have been dominantly derived by metamorphic processes in a source zone at depth within the rift down dip and beneath the native copper deposits.
2. The variability and absolute values of the oxygen and carbon isotopic composition of the hydrothermal fluids are not easily explained by fluids derived by metamorphic processes alone. The data are consistent with mixing of evolved seawater and evolved meteoric water with metamorphic derived fluids.
3. The evolved seawater, depleted in sulfur prior to burial metamorphism, participated with burial metamorphic derived fluids at depth in the source zone, wherein it became part of a well-mixed hybrid ore-forming fluid. The evolved seawater provided a significant amount of salinity to the ore-forming fluid.
4. The hybrid ore-forming fluids moved upward into the zone of precipitation where they mixed with sulfur-poor, reduced evolved meteoric water. The evolved meteoric water was one factor that facilitated precipitation of native copper from the hybrid ore-forming fluid. Incomplete mixing of evolved meteoric waters with hybrid ore-forming fluids in the zone of precipitation resulted in carbon isotopic heterogeneity at the mm scale within growth zoned calcite crystals as documented through spot isotopic analyses by SIMS.
5. Co-variation of oxygen and carbon isotopic compositions of late-stage hydrothermal fluids is different than for main-stage hydrothermal fluids. Main-stage hybrid ore-forming fluids are a lesser component of the late-stage hydrothermal fluids consistent

with the late-stage hydrothermal activity being a continuum with main-stage activity. The late-stage hydrothermal fluids are mostly composed of evolved meteoric water and shallow evolved seawater.

This oxygen and carbon isotope study provides new insight into and confirmation of the existing genetic model of the native copper deposits of the Keweenaw Peninsula. The oxygen and carbon isotopic composition of hydrothermal fluids calculated from calcite cannot provide definitive conclusions, but it is of value when integrated with other data and inferences. The genetic model would benefit from additional light stable isotope studies.

Supplementary Materials: The analytical data can be downloaded at: <https://www.mdpi.com/article/10.3390/min12040474/s1>. Table S1: Main-stage stable isotope bulk calcite data from the Kearsarge deposit. Table S2: Main-stage stable isotope SIMS calcite data for sample TB-293. Table S3: Late-stage stable isotope SIMS calcite data for sample WAS-121. Table S4: Main-stage stable isotope SIMS calcite data sample WAS752. Table S5: Main-stage stable isotope SIMS calcite data for sample WAS-505. Table S6: Main-stage stable isotope SIMS calcite data for sample CAL-94-29. Table S7: Main-stage stable isotope SIMS calcite data for sample MOR-1. Table S8: Main-stage stable isotope SIMS calcite data for sample DK-1. Table S9: Late-stage stable isotope SIMS calcite data for sample CM-1. Figure S1: Spot Analysis Cathodoluminescence image of TB-293. Figure S2: Spot Analysis Cathodoluminescence image of WAS-121. Figure S3: Spot Analysis Cathodoluminescence image of WAS-752. Figure S4: Spot analysis cathodoluminescence image of WAS-505. Figure S5: Spot analysis cathodoluminescence image of CAL-94-29. Figure S6: Spot analysis cathodoluminescence image of MOR-1. Figure S7: Spot analysis cathodoluminescence images of DK-1a and DK-1b. Figure S8: Spot Analysis Cathodoluminescence images of CM-1a, CM-1b, and CM-1c.

Author Contributions: This paper is an extension of the MSc thesis of T.J.B. (Thomas J. Bodden) at Michigan Tech co-supervised by T.J.B. (Theodore J. Bornhorst), C.D. and F.B. performed the new SIMS analytical work published in T.J.B. (Thomas J. Bodden) and additional data published herein. She served on T.J.B. (Thomas J. Bodden) examining committee. T.J.B. (Theodore J. Bornhorst) wrote the paper and developed the interpretations with assistance from T.J.B. (Thomas J. Bodden), F.B. and C.D. provided significant contributions in assisting in interpretations and during the preparation of this paper. All authors have read and agreed to the published version of the manuscript.

Funding: This work was supported by the A. E. Seaman Mineral Museum's Edith Dunn and E. Wm. Heinrich Mineralogical Research Trust, Michigan Tech and the Department of Geological and Mining Engineering and Sciences of Michigan Tech. Bodden received a student research grant from the Institute on Lake Superior Geology.

Data Availability Statement: New data are available in the Supplementary Materials.

Acknowledgments: We thank the A. E. Seaman Mineral Museum of Michigan Tech for providing samples used for the SIMS analyses, and Anne Sophie Bouvier and Florent Plane for technical support at the Swiss SIMS facility. This work was motivated by an earlier collaboration between Bornhorst and Laurel Woodruff, U.S. Geological Survey. This paper benefited from discussion over the years with Laurel.

Conflicts of Interest: The authors declare no conflict of interest.

References

1. Weege, R.J.; Pollack, J.P. Recent developments in native-copper district of Michigan. In Proceedings of the Society of Economic Geologists Guidebook for Field Conference, Houghton, MI, USA, 30 September–2 October 1971; pp. 19–43.
2. Bornhorst, T.J.; Lankton, L.D. Copper mining: A billion years of geologic and human history. In *Michigan Geography and Geology*; Schaetzl, R., Darden, J., Brandt, D., Eds.; Pearson Custom Publishing: New York, NY, USA, 2009; pp. 150–173.
3. Walin, H. *Douglass Houghton Michigan's First State Geologist 1837–1845: Michigan Geological and Land Management Division Pamphlet 1*; Department of Environmental Quality: Richmond, VA, USA, 2004; p. 20.
4. Butler, B.S.; Burbank, W.S. The copper deposits of Michigan. *U.S. Geol. Surv. Prof. Pap.* **1929**, *144*, 1–238.
5. White, W.S. The native-copper deposits of northern Michigan. In *Ore Deposits of the United States, 1933–1967 (Graton Sales Volume)*; Ridge, J.D., Ed.; American Institute of Mining, Metallurgical, and Petroleum Engineers: New York, NY, USA, 1968; pp. 303–325.
6. Livnat, A. Metamorphism and Copper Mineralization of the Portage Lake Lava Series, Northern Michigan. Ph.D. Thesis, University of Michigan, Ann Arbor, MI, USA, 1983; pp. 1–292.

7. Püschner, U.R. Very low-grade metamorphism in the Portage Lake Volcanics on the Keweenaw Peninsula, Michigan, USA. Ph.D. Thesis, University of Basel, Basel, Switzerland, 2001; pp. 1–81.
8. Jolly, W.T. Behavior of Cu, Zn, and Ni during prehnite-pumpellyite rank metamorphism of the Keweenaw basalts, northern Michigan. *Econ. Geol.* **1974**, *69*, 1118–1125. [[CrossRef](#)]
9. Jolly, W.T.; Smith, R.E. Degradation and metamorphic differentiation of the Keweenaw tholeiitic lavas of northern Michigan, USA. *J. Petrol.* **1972**, *13*, 273–309. [[CrossRef](#)]
10. Bornhorst, T.J.; Woodruff, L.G. Native copper precipitation by fluid-mixing Keweenaw Peninsula, Michigan. *Inst. Lake Super. Geol. Proc.* **1997**, *4 Pt 1*, 9–10.
11. Cannon, W.F.; Green, A.G.; Hutchinson, D.R.; Lee, M.W.; Milkereit, B.; Behrendt, J.C.; Halls, H.C.; Green, J.C.; Dickas, A.B.; Morey, G.B.; et al. The North American mid-continent rift beneath Lake Superior from Glimpse seismic reflection profiling. *Tectonics* **1989**, *8*, 305–332. [[CrossRef](#)]
12. Heaman, L.M.; Easton, R.M.; Hart, T.M.; MacDonald, C.A.; Hollings, P.; Smyk, M. Further refinement to the timing of Mesoproterozoic magmatism, Lake Nipigon region, Ontario. *Can. J. Earth Sci.* **2007**, *44*, 1055–1086. [[CrossRef](#)]
13. Hodgin, E.B.; Swanson-Hysell, N.L.; DeGraff, J.M.; Kylander-Clark, A.R.C.; Schmitz, M.D.; Turner, A.C.; Zhang, Y.; Stolper, D.A. Final Inversion of the Mid-Continent Rift during the Rigolet Phase of the Grenvillian Orogeny. *Geology* **2022**, *in press*.
14. Davis, D.W.; Paces, J.B. Time resolution of geologic events on the Keweenaw Peninsula and implications for development of the Midcontinent Rift system. *Earth Planet. Sci. Lett.* **1990**, *97*, 54–64. [[CrossRef](#)]
15. Davis, D.W.; Green, J.C. Geochronology of the North American Midcontinent rift in western Lake Superior and implications for its geodynamic evolution. *Can. J. Earth Sci.* **1997**, *34*, 476–488. [[CrossRef](#)]
16. Merk, G.P.; Jirsa, M.A. *Provenance and Tectonic Significance of the Keweenaw Interflow Sedimentary Rocks*; The Geological Society of America: Boulder, CO, USA, 1982; pp. 97–106.
17. Nicholson, S.W. Geochemistry, petrography, and volcanology of rhyolites of the Portage Lake Volcanics, Keweenaw Peninsula, Michigan. *U.S. Geol. Surv. Bull.* **1992**, *1970*, B1–B57.
18. Bodden, T.J. Spatial and Temporal Distribution of Hydrothermal Minerals and Sources of Hydrothermal Minerals Inferred from Light Stable Isotopes, Keweenaw Peninsula Native Copper District, Michigan. Master's Thesis, Michigan Technological University, Houghton, MI, USA, 2019; pp. 1–87.
19. Kalliokoski, J. Calcium carbonate cement (caliche) in Keweenaw sedimentary rocks (~1.1 Ga) Upper Peninsula of Michigan. *Precambrian Res.* **1986**, *32*, 243–259. [[CrossRef](#)]
20. Elmore, R.D. The Copper Harbor Conglomerate: A late Precambrian fining-upward alluvial fan sequence in northern Michigan. *Geol. Soc. Am. Bull.* **1984**, *95*, 610–617. [[CrossRef](#)]
21. Bornhorst, T.J.; Williams, W.C. The Mesoproterozoic Copperwood Sedimentary Rock-Hosted Stratiform Copper Deposit, Upper Peninsula, Michigan. *Econ. Geol.* **2013**, *108*, 1325–1346. [[CrossRef](#)]
22. Ohr, M. Geochronology of Diagenesis and Low-Grade Metamorphism in Pelites. Ph.D. Thesis, The University of Michigan, Ann Arbor, MI, USA, 1993.
23. Jones, S.; Prave, A.R.; Raub, T.D.; Cloutier, J.; Stüeken, E.E.; Rose, C.V.; Linnekogel, S.; Nazarov, K. A marine origin for the late Mesoproterozoic Copper Harbor and Nonesuch Formations of the Midcontinent Rift of Laurentia. *Precambrian Res.* **2020**, *336*, 105510. [[CrossRef](#)]
24. Stüeken, E.E.; Jones, S.; Raub, T.D.; Prave, A.R.; Rose, C.V.; Linnekogel, S.; Cloutier, J. Geochemical fingerprints of seawater in the Late Mesoproterozoic Midcontinent Rift, North America: Life at the marine-land divide. *Chem. Geol.* **2020**, *553*, 119812. [[CrossRef](#)]
25. Kulakov, E.; Bornhorst, T.J.; Deering, C.; Moore, J. The youngest magmatic activity of the Midcontinent Rift at Bear Lake, Keweenaw Peninsula, Michigan. *Inst. Lake Super. Geol. Proc.* **2018**, *64 Pt 1*, 61–62.
26. Cannon, W.F. Closing of the Midcontinent Rift—A far field effect of Grenvillian contraction. *Geology* **1994**, *22*, 155–158. [[CrossRef](#)]
27. Cannon, W.F.; Peterman, Z.E.; Sims, P.K. Crustal-scale thrusting and origin of the Montreal River monocline—A 35-km-thick cross section of Midcontinent Rift in northern Michigan and Wisconsin. *Tectonics* **1993**, *12*, 728–744. [[CrossRef](#)]
28. Bornhorst, T.J. Maximum depositional age of the Neoproterozoic Jacobsville Sandstone, Michigan: Implications for the evolution of the Midcontinent Rift: COMMENT. *Geosphere* **2018**, *14*, 1380–1381. [[CrossRef](#)]
29. Bornhorst, T.J.; Mathur, R. Copper isotope constraints on the genesis of the Keweenaw Peninsula native copper district, Michigan, USA. *Minerals* **2017**, *7*, 185. [[CrossRef](#)]
30. Bornhorst, T.J.; Paces, J.B.; Grant, N.K.; Obradovich, J.D.; Huber, N.K. Age of native copper mineralization, Keweenaw Peninsula, Michigan. *Econ. Geol.* **1988**, *83*, 619–625. [[CrossRef](#)]
31. Schmidt, S.T.; Süssenberger, A.; Wemmer, K. Post-eruptive thermal history of the Proterozoic Basaltic North Shore Volcanic Group of the Midcontinent Rift: Evidence from K/Zr Data of Celadonite. *Lithosphere* **2021**, *2021*, 18. [[CrossRef](#)]
32. Ruiz, J.; Jones, L.M.; Kelly, W.C. Rubidium-strontium dating of ore deposits hosted by Rb-rich rocks, using calcite and other common Sr-bearing minerals. *Geology* **1984**, *12*, 259–262. [[CrossRef](#)]
33. Bornhorst, T.J. Tectonic context of native copper deposits of the North American Midcontinent Rift system. *Geol. Soc. Am. Spec. Pap.* **1997**, *312*, 127–136.
34. Stoiber, R.E.; Davidson, E.S. Amygdule mineral zoning in the Portage Lake Lava Series, Michigan copper district. *Econ. Geol.* **1959**, *54*, 1250–1277. [[CrossRef](#)]

35. Bornhorst, T.J.; Suchoski, J.P. A physicochemical model for the deposition of native copper and associated minerals in the Keweenaw Peninsula native copper district, Michigan. In Proceedings of the International Field Conference and Symposium, IGCP Project 336, Duluth, MN, USA, 22–31 August 1995; pp. 19–20.
36. Schmidt, S.T.; Robinson, D. Metamorphic grade and porosity and permeability controls on mafic phyllosilicate distributions in a regional zeolite to greenschist facies transition of the North Shore Volcanic Group, Minnesota. *Geol. Soc. Am. Bull.* **1997**, *109*, 683–697. [[CrossRef](#)]
37. McCrea, J.M. On the isotope chemistry of carbonates and a paleotemperature scale. *J. Chem. Phys.* **1950**, *18*, 849–857. [[CrossRef](#)]
38. Bégué, F.; Baumgartner, L.P.; Bouvier, A.S.; Robyr, M. Reactive fluid infiltration along fractures: Textural observations coupled to in-situ isotopic analyses. *Earth Planet. Sci. Lett.* **2019**, *519*, 264–273. [[CrossRef](#)]
39. Linzmeier, B.; Kitajima, K.; Denny, A.; Cammack, J. Making maps on a micrometer scale. *Eos* **2018**, *99*, 1–8. [[CrossRef](#)]
40. O’Neil, J.R.; Clayton, R.N.; Mayeda, T.K. Oxygen isotope fractionation in divalent metal carbonates. *J. Chem. Phys.* **1969**, *51*, 5547–5558. [[CrossRef](#)]
41. Friedman, I.; O’Neil, J.R. Compilation of stable isotope fractionation factors of geochemical interest. In *Data of Geochemistry*, 6th ed.; U.S. Government Publishing Office: Washington, DC, USA, 1977; pp. 13–59.
42. Sheele, N.; Hoefs, J. Carbon isotope fractionation between calcite, graphite and CO₂: An experimental study. *Contrib. Mineral. Petrol.* **1992**, *112*, 35–45. [[CrossRef](#)]
43. Ohmoto, H. Systematics of Sulfur and Carbon Isotopes in Hydrothermal Ore Deposits. *Econ. Geol.* **1972**, *16*, 551–578. [[CrossRef](#)]
44. Bornhorst, T.J.; Mathur, R. Copper isotope constraints on the Genesis of the Keweenaw Peninsula Native Copper District, Michigan, USA: Reply. *Minerals* **2018**, *8*, 508. [[CrossRef](#)]
45. Woodruff, L.G.; Daines, M.J.; Cannon, W.F.; Nicholson, S.W. The thermal history of the Midcontinent Rift in the Lake Superior region: Implications for mineralization and partial melting. In Proceedings of the International Geological Correlation Program, Field Conference and Symposium on the Petrology and Metallogeny of Volcanic and Intrusive Rocks of the Midcontinent Rift System, Duluth, MN, USA, 22–31 August 1995; Volume 336, pp. 213–214.
46. Cornwall, H.R. A summary of ideas on the origin of native copper deposits. *Econ. Geol.* **1956**, *51*, 615–631. [[CrossRef](#)]
47. Paces, J.B.; Miller, J.D., Jr. Precise U-Pb ages of the Duluth Complex and related mafic intrusions, northeastern, Minnesota: New insights for physical, petrogenetic, paleomagnetic and tectono-magmatic processes associated with 1.1 Ga Midcontinent rifting. *J. Geophys. Res.* **1993**, *98*, 13997–14013. [[CrossRef](#)]
48. Kelly, D. Fluid Inclusion Study of Selected Calcite Associated with Native Copper, Quincy Mine, Keweenaw Peninsula, Michigan. Master’s Thesis, Michigan Technological University, Houghton, MI, USA, 2020; p. 65.
49. Brown, A.C. District-scale concentration of native copper lodes from a tectonically induced thermal plume of ore fluids on the Keweenaw Peninsula, Northern Michigan. *Econ. Geol.* **2008**, *103*, 1691–1694. [[CrossRef](#)]
50. Brown, A.C. Genesis of native copper lodes in the Keweenaw Peninsula, Northern Michigan: A hybrid evolved meteoric and metamorphogenic model. *Econ. Geol.* **2006**, *101*, 1437–1444. [[CrossRef](#)]
51. Sharp, Z. *Principles of Stable Isotope Geochemistry*, 2nd ed.; University of New Mexico: Albuquerque, NM, USA, 2017. [[CrossRef](#)]
52. Bornhorst, T.J. Evolved seawater as the source for metamorphic-dominated ore-forming hydrothermal fluids of the Keweenaw Peninsula native copper district, Michigan. *Inst. Lake Super. Geol. Proc.* **2021**, *67 Pt 1*, 5–6.
53. Antonelli, M.A.; Pester, N.J.; Brown, S.T.; DePaolo, D.J. Effect of paleoseawater composition on hydrothermal exchange in midocean ridges. *Proc. Natl. Acad. Sci. USA* **2017**, *114*, 12413–12418. [[CrossRef](#)]
54. Tivey, M.K. Generation of seafloor hydrothermal vent fluids and associated mineral deposits. *Oceanography* **2007**, *20*, 50–65. [[CrossRef](#)]
55. Hardie, L.A. The roles of rifting and hydrothermal CaCl₂ brines in the origin of potash evaporites: An hypothesis. *Am. J. Sci.* **1990**, *290*, 43–106. [[CrossRef](#)]
56. Blättler, C.L.; Bergmann, K.D.; Kah, L.C.; Gómez-Pérez, I.; Higgins, J.A. Constraints on Meso-Neoproterozoic seawater from ancient evaporite deposits. *Earth Planet. Sci. Lett.* **2020**, *532*, 115951. [[CrossRef](#)]
57. Taylor, H.P., Jr. Oxygen and hydrogen isotope relationships in hydrothermal mineral deposits. In *Geochemistry of Hydrothermal Ore Deposits*; Barnes, H.L., Ed.; John and Wiley and Sons: New York, NY, USA, 1997; pp. 228–302.
58. Park, Y.-R.; Ripley, E.M. Hydrothermal flow systems in the Midcontinent Rift: Oxygen and hydrogen isotopic studies of the North Shore Volcanic Group and related hypabyssal sills, Minnesota. *Geochim. Cosmochim. Acta* **1999**, *63*, 1787–1804. [[CrossRef](#)]
59. Baumgartner, L.P.; Valley, J.W. Stable Isotope Transport and Contact Metamorphic Fluid Flow. *Rev. Miner. Geochem.* **2001**, *43*, 415–467. [[CrossRef](#)]
60. Schlesinger, W.H.; Marion, G.M.; Fonteyn, P.J. Stable Isotopes in Ecological Research. In *Stable Isotope Ratios and the Dynamics of Caliche in Desert Soils*; Rundel, P.W., Ehleringer, J.R., Nagy, K.A., Eds.; Springer: Berlin/Heidelberg, Germany, 1989; pp. 309–317.
61. Kalliokoski, J.; Welch, E.J. Keweenaw-age caliche paleosol in the lower part of the Calumet and Hecla Conglomerate, Centennial mine, Calumet, Michigan. *Geol. Soc. Am.* **1985**, *96*, 1188–1193. [[CrossRef](#)]
62. Knauth, L.P.; Mauro, B.; Klonowski, S. Isotope geochemistry of caliche developed on basalt. *Geochim. Cosmochim. Acta* **2003**, *67*, 185–195. [[CrossRef](#)]